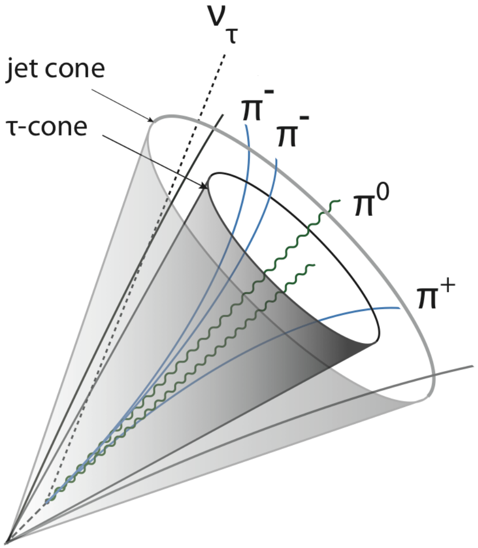

Reconstruction of Tau Leptons and Applications in the ATLAS Experiment

Peter Wagner
Uni Bonn

universitätbonn

BMBF-Forschungsschwerpunkt
ATLAS-EXPERIMENT
Physik bei höchsten Energien mit dem ATLAS-Experiment am LHC

FSP 103
ATLAS

Overview

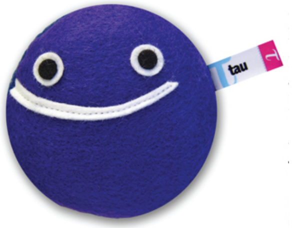

- The tau lepton, LHC and ATLAS
- Higgs analysis with taus
- New: Particle Flow
- What do we gain from it?

The Tau Lepton

- Mass ~ 1.8 GeV
- Proper decay length: ~ 87 μm
- Weak decays:

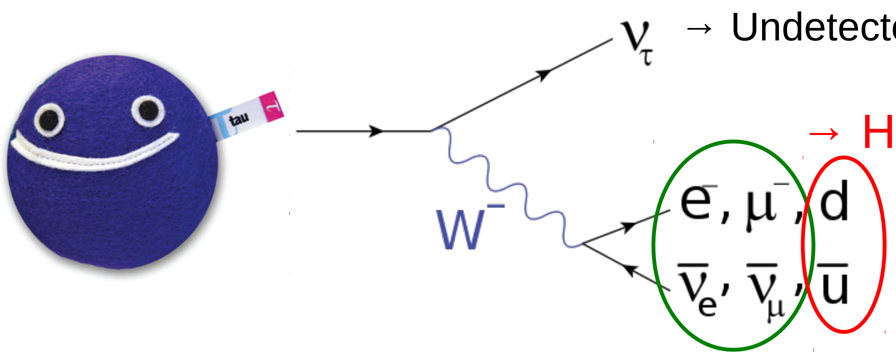

→ Undetected

→ Hadronic modes

→ Leptonic modes

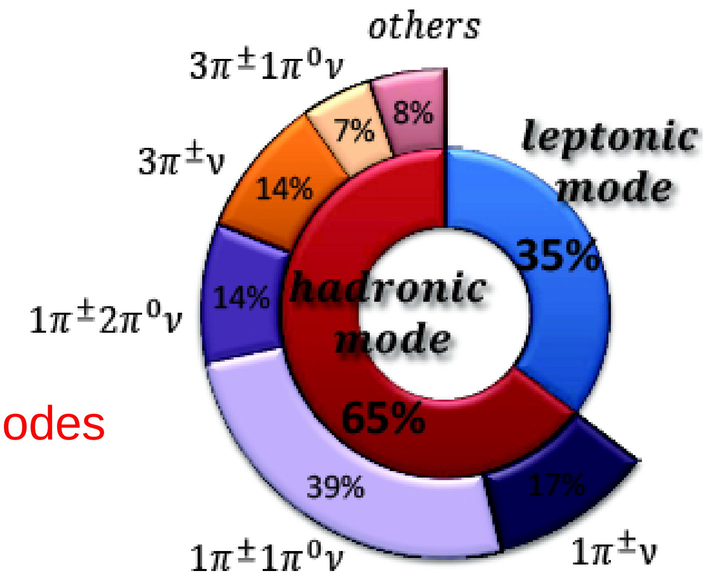

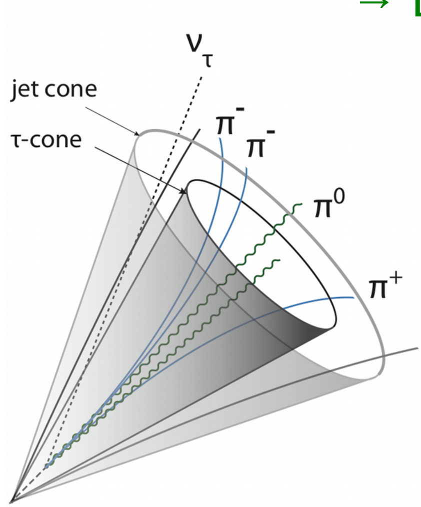

In the ATLAS detector:

- Leptonic decays really “look like” e,μ
- “Tau” = hadronic decay

LHC – Our Source of τ Leptons

- LHC collides protons
- “Run 1” completed in Feb 2013: collision energy of 7 and 8 TeV
- “Run 2” started 2015: 13 TeV collision energy, more integrated luminosity

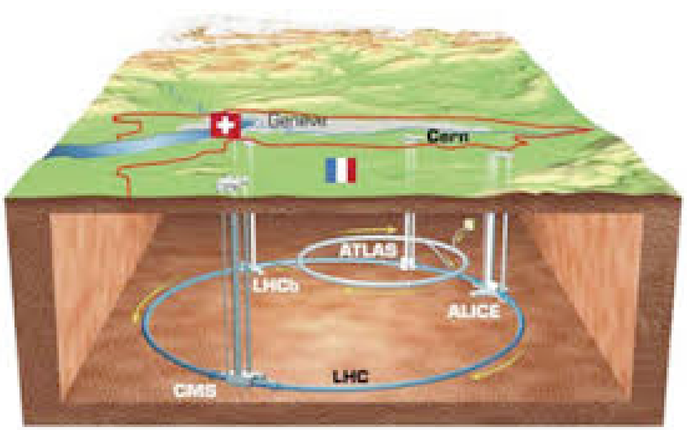

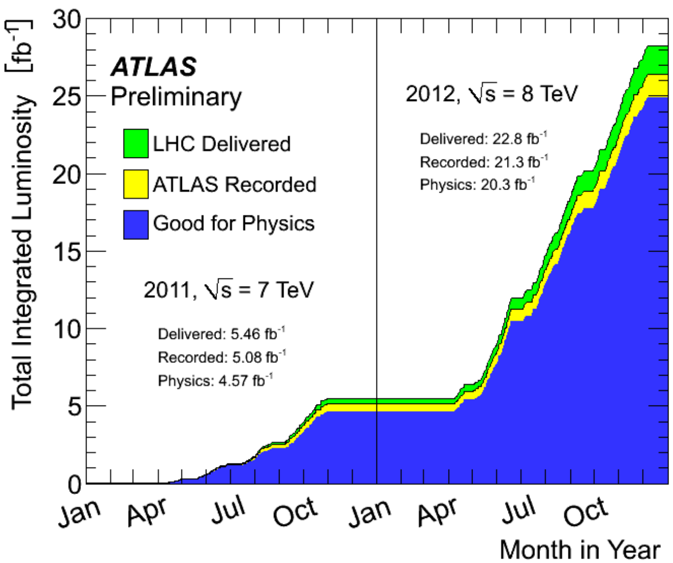

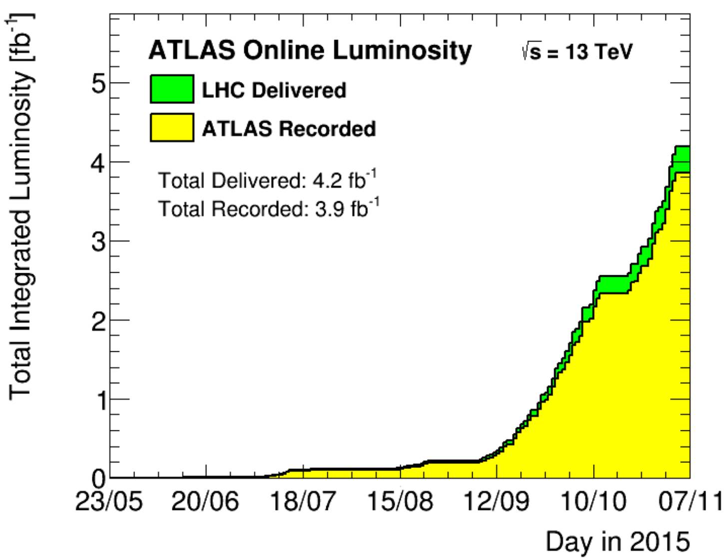

LuminosityPublicResults

ATLAS Detector

- Multi-purpose detector for various physics signatures with leptons, jets, photons
- Momentum range ~1-1000 GeV (typically 10-100 GeV from EW processes)
- 2T magnetic field

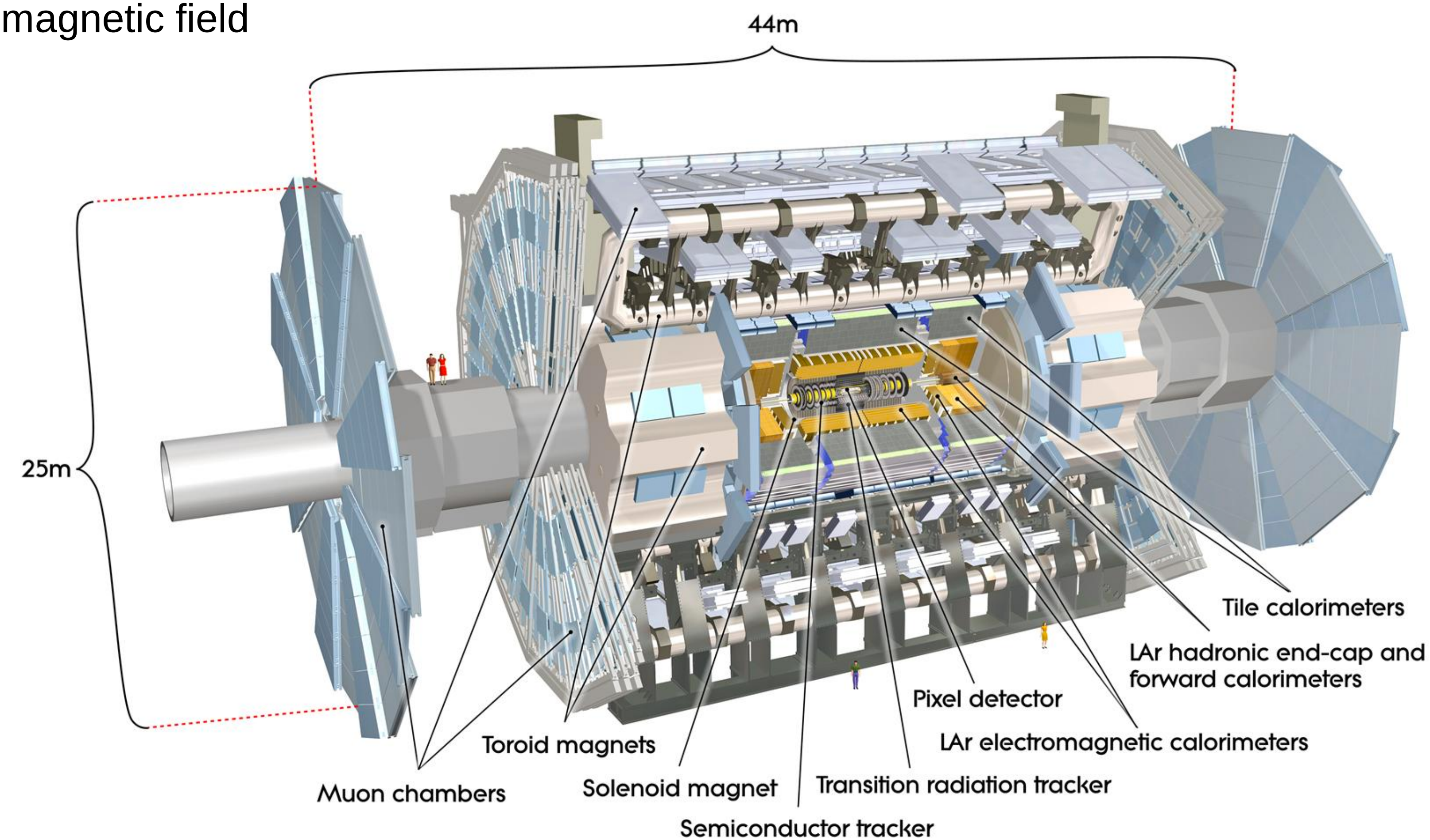

ATLAS Detector

Detection:

- Charged particles: Tracking detectors, $\sigma/p_T \sim 0.05\% \cdot p_T$[GeV] resolution
- e,γ: EM calorimeters: $\sigma/E \sim 10\%/\sqrt{E[GeV]}$
- Hadronic calorimeter: $\sigma/E \sim 50\%/\sqrt{E[GeV]}$
- Muon spectrometer: $\sigma/p < 10\%$

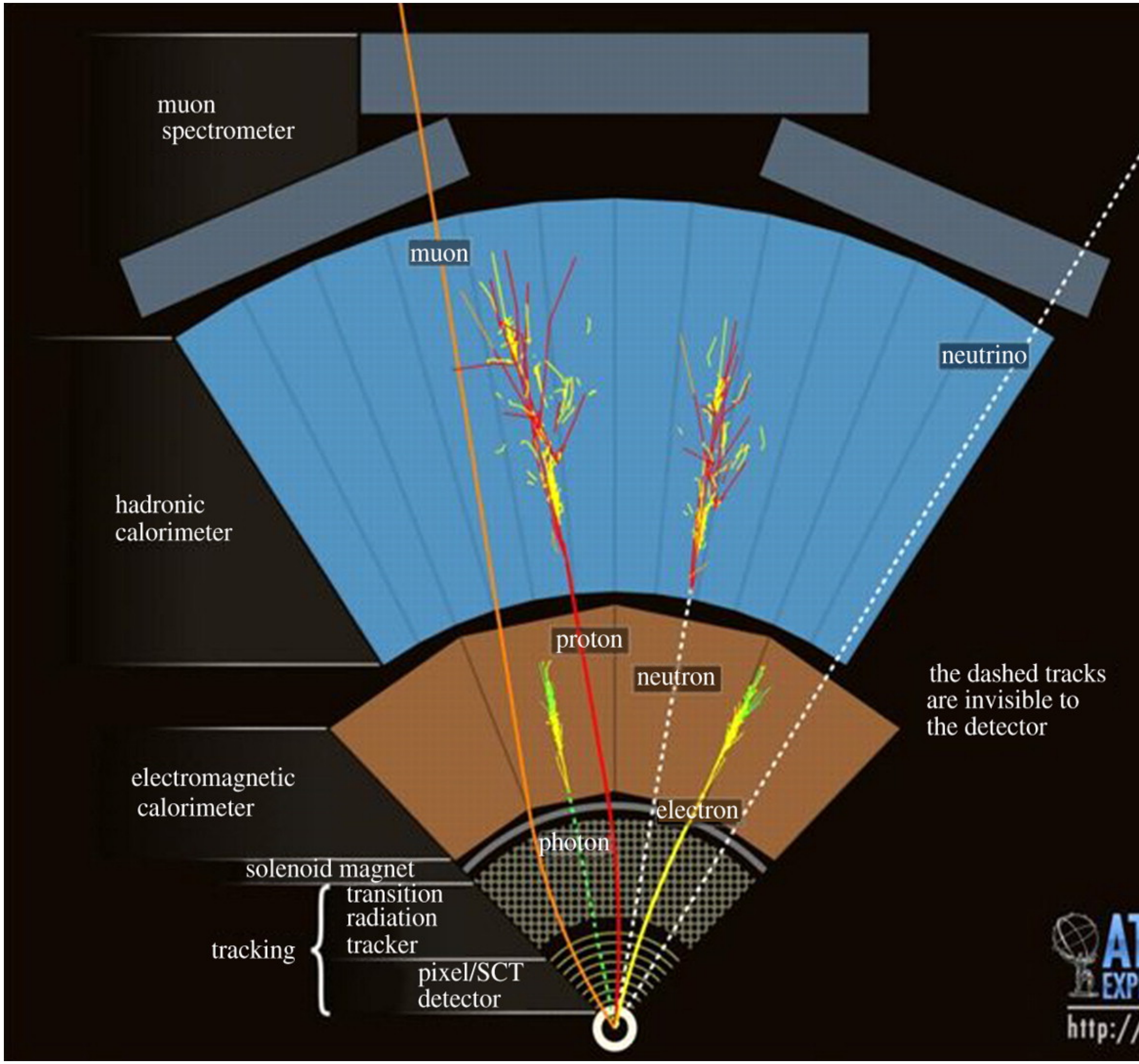

Run 1 Higgs Discovery

"Higgs boson" discovery in 2012 from combined analysis of multiple decay channels: γγ, ZZ, WW

$H \rightarrow \tau\tau$: 4.5σ excess observed

- SM Higgs-to-lepton coupling largest for τ → only accessible fermionic decay channel so far
- Evidence for Yukawa couplings of Higgs
- Strong constraints on VBF production cross section

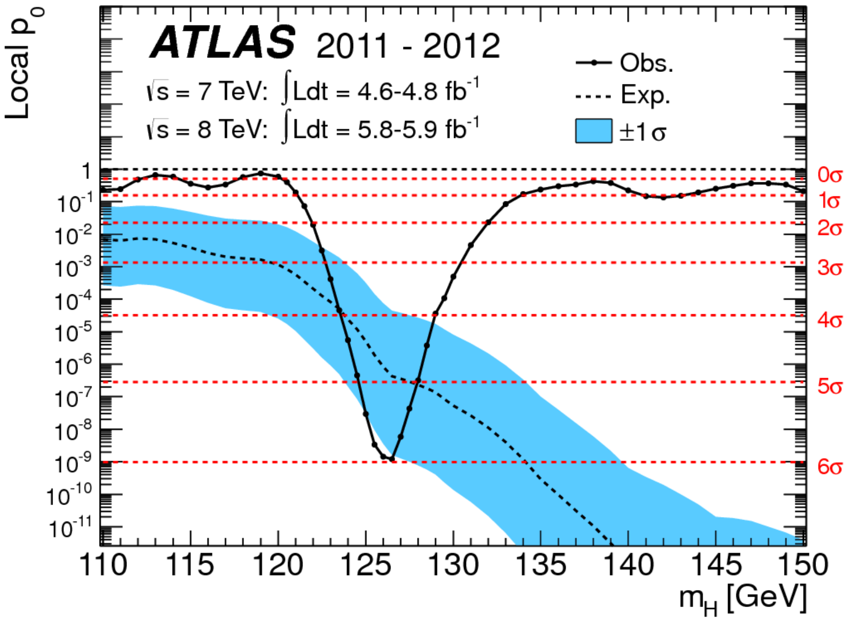

Phys Lett B 716 (2012) 1

JHEP 04 (2015) 117

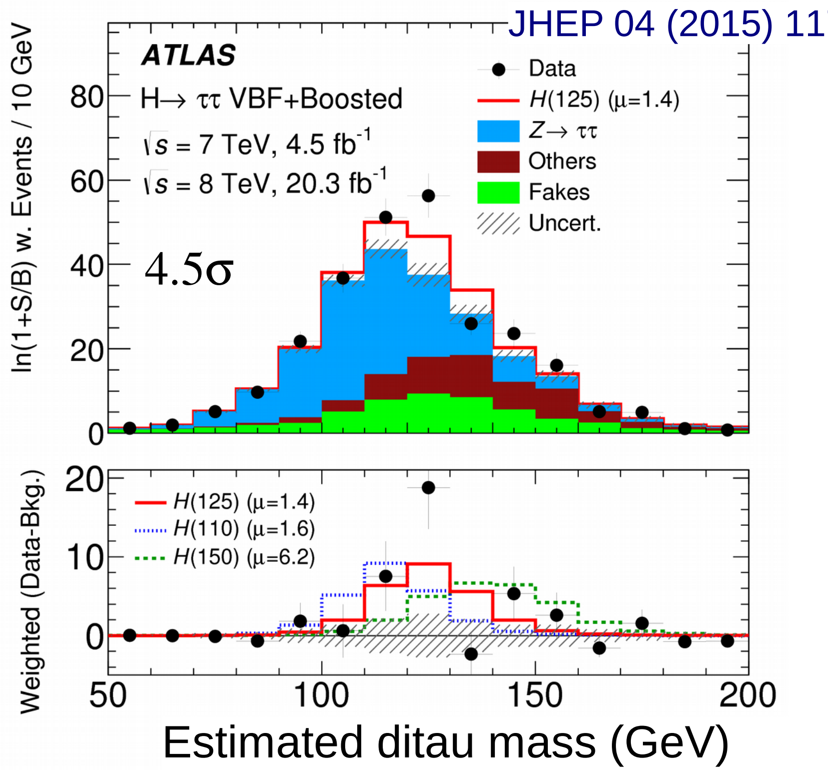

Higgs analysis with τ's – Requirements

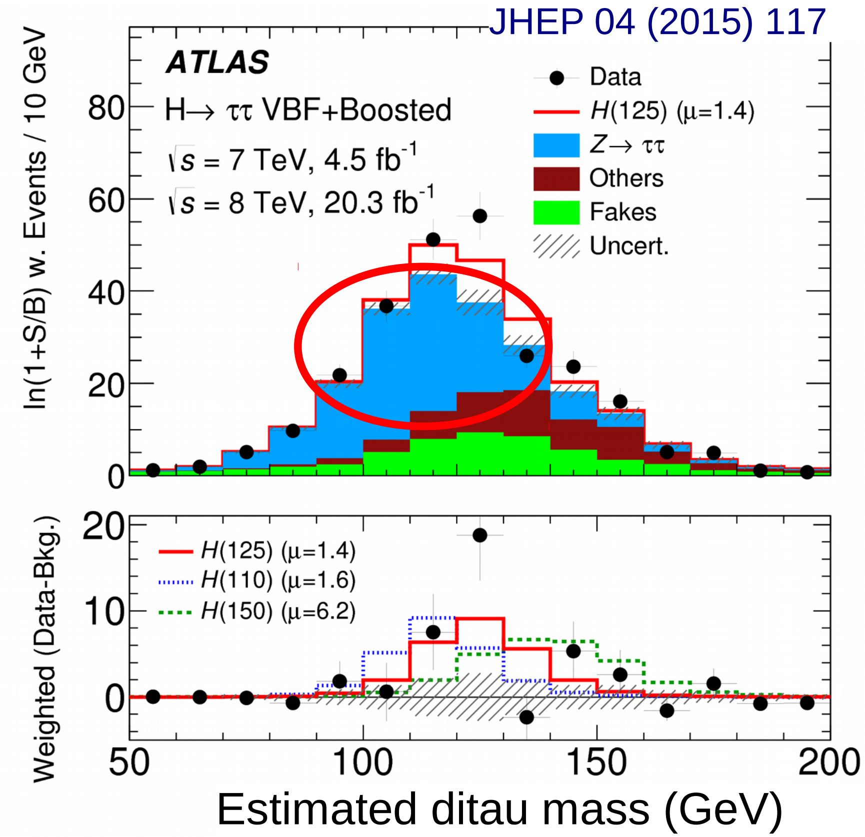

Real τ's major background to H → ττ signal:

Broad ditau mass peak due to invisible ν's, difficult to reconstruct

⇒

- Need good kinematic discrimination
- Good 4-momentum resolution of visible τ helps here!

Taus in the ATLAS Calorimeter

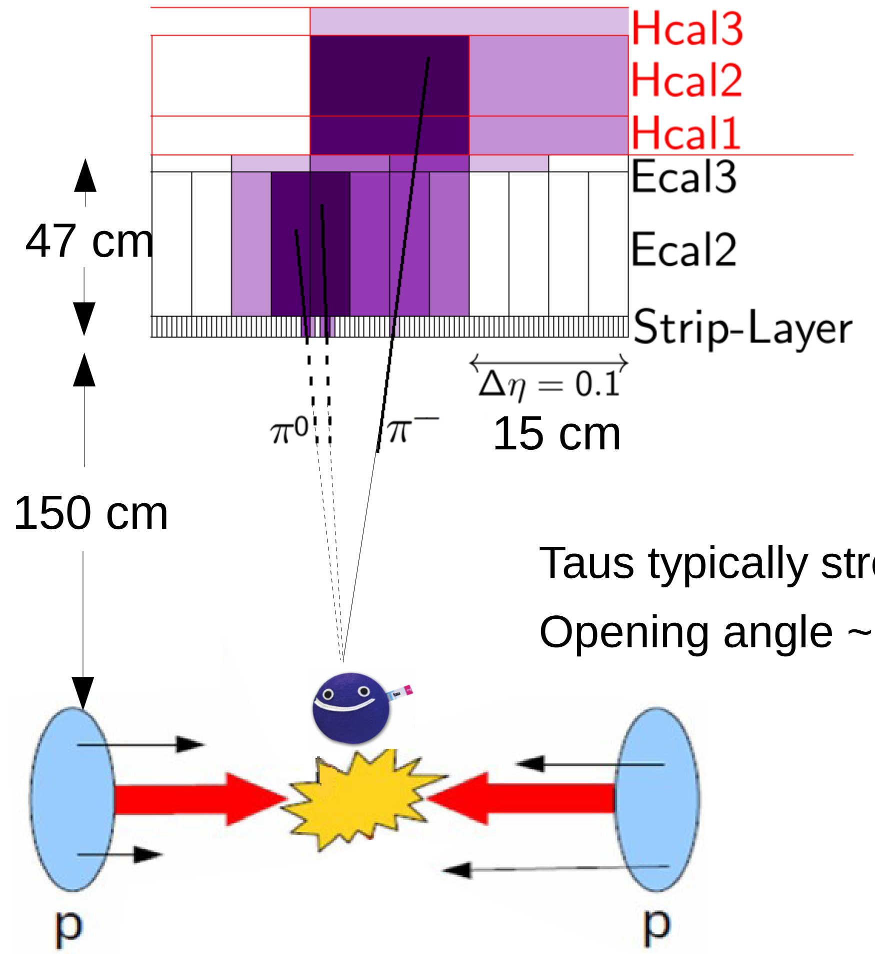

Taus typically strongly boosted:

Opening angle ~ 0.2 rad

Taus in the ATLAS Calorimeter

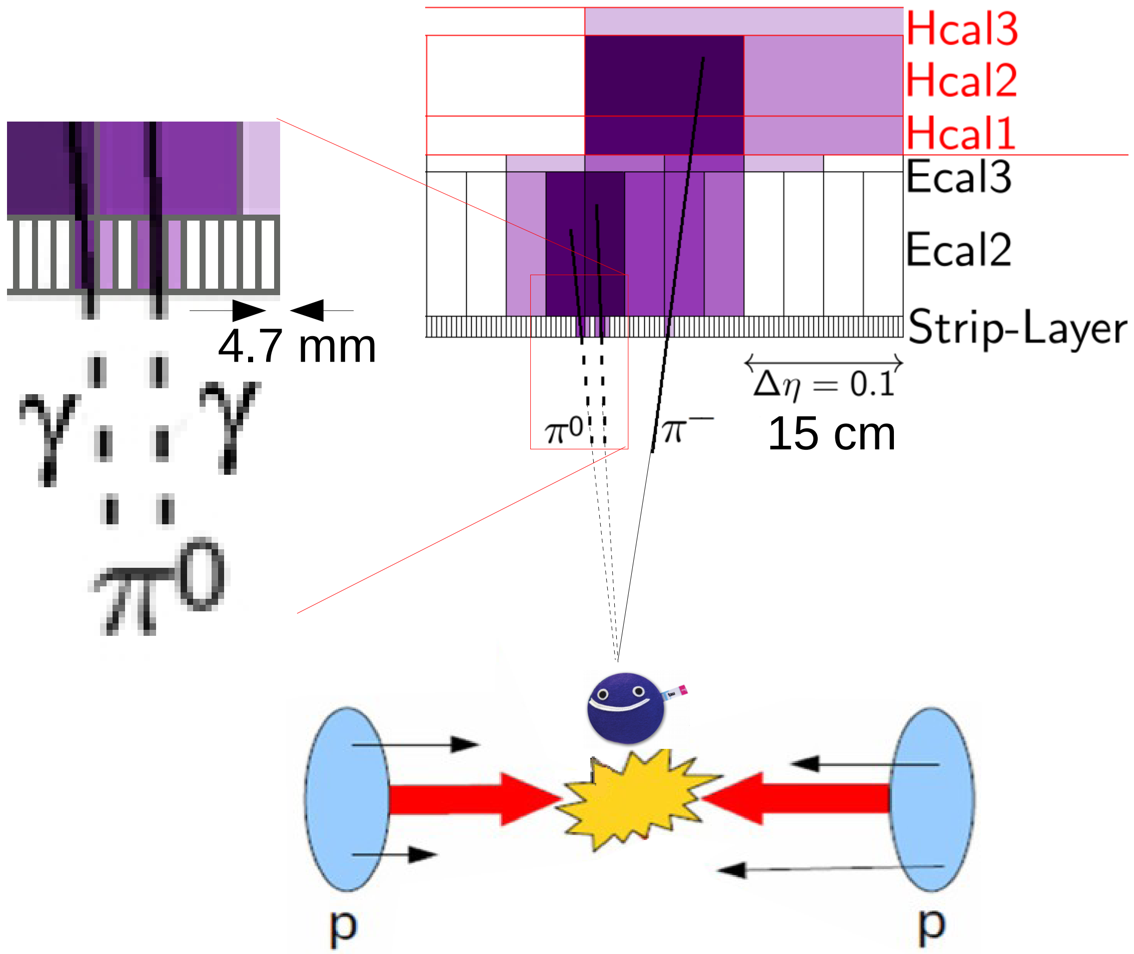

Run 1 Energy Measurement

Run 1: visible τ energy measured entirely in the calorimeter:

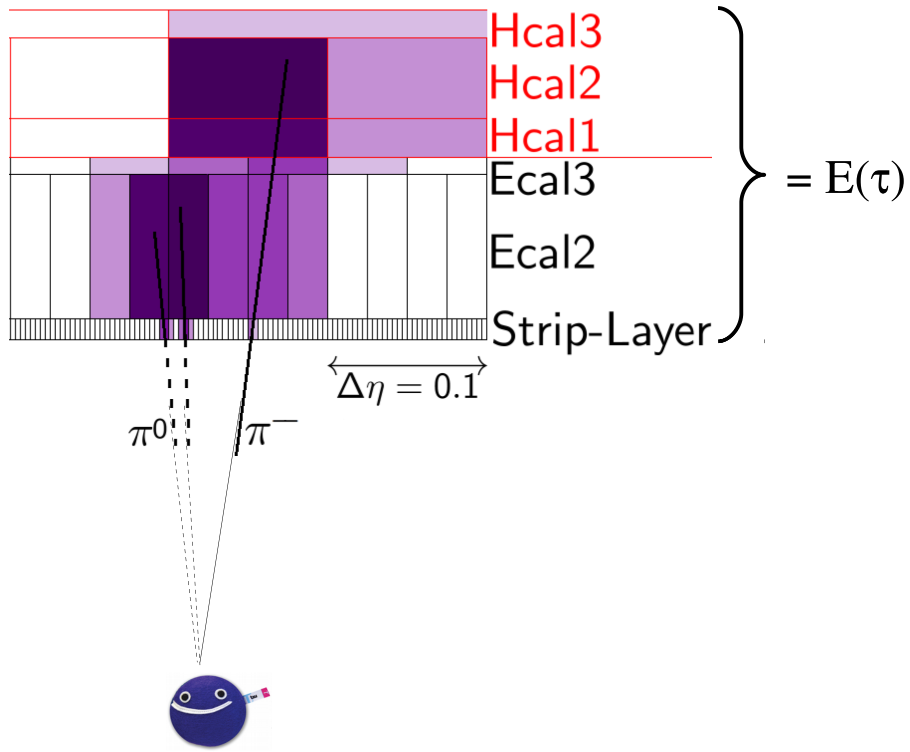

Run 1 Energy Measurement

Run 1: visible τ energy measured entirely in the calorimeter:

However poor calorimeter resolution of $\pi^{\pm}$ limits energy resolution, e.g. HCAL:

$$\frac{\sigma(E)}{E} \approx \frac{50\%}{\sqrt{E}} \oplus 3\%$$

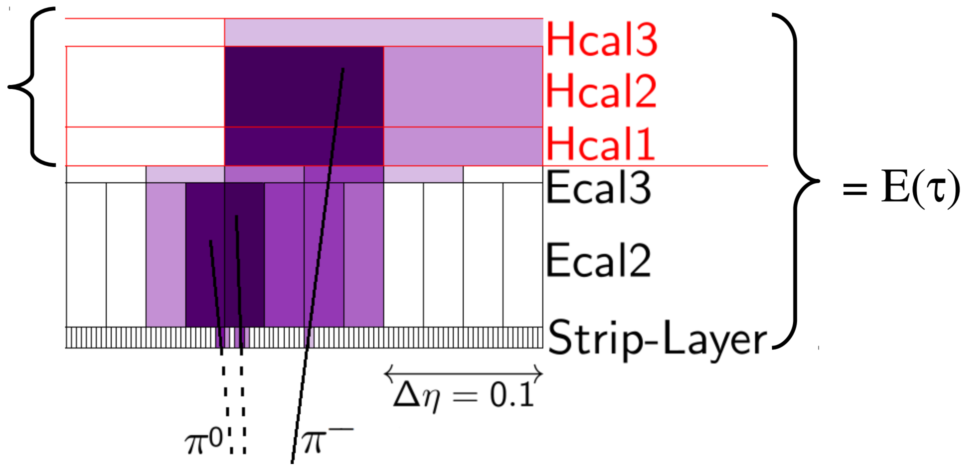

Run 1 Energy Measurement

Run 1: visible τ energy measured entirely in the calorimeter:

However poor calorimeter resolution of $\pi^{\pm}$ limits energy resolution, e.g. HCAL:

$$\frac{\sigma(E)}{E} \approx \frac{50\%}{\sqrt{E}} \oplus 3\%$$

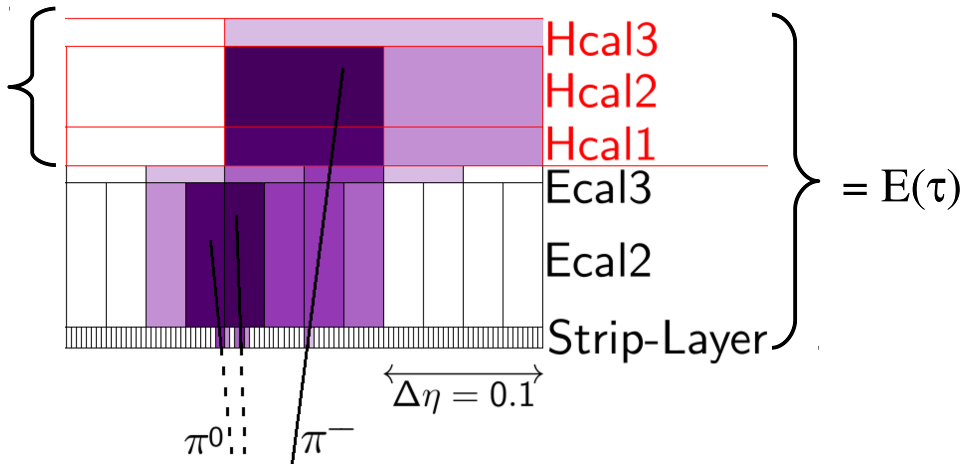

Energy resolution of $\pi^{\pm}$ is superior in the tracker below p_T ~ 120 GeV

→ Can do better than Run 1 method!

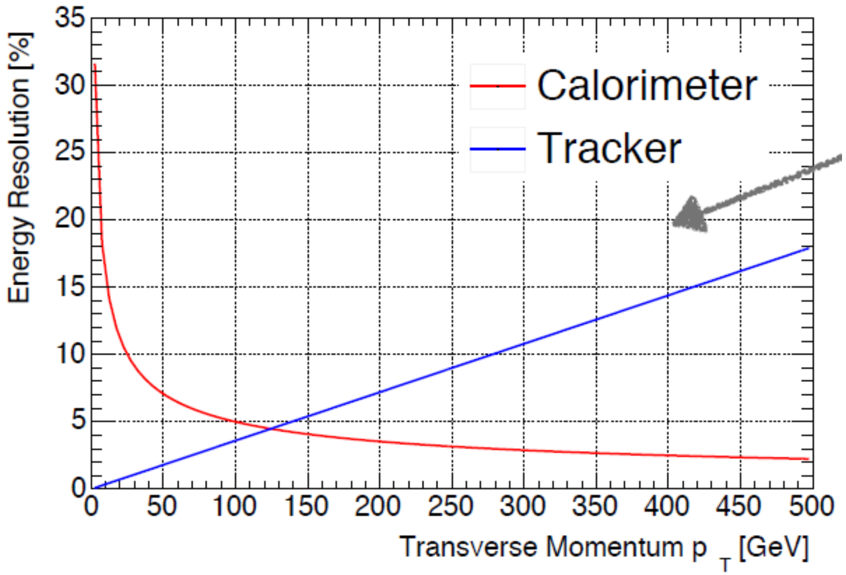

New for Run 2 @ ATLAS: Particle Flow

Alternative: "Particle Flow" approach

"Exploit full detector information to resolve, identify and measure each single particle!"

- No strict definition – move away from pure calorimetry for 4-momentum measurements
- Measure 4-momentum with tracking detector instead of calorimeter → improve resolution!
- For both isolated and non-isolated particles! e.g. inside jet or hadronically decaying tau

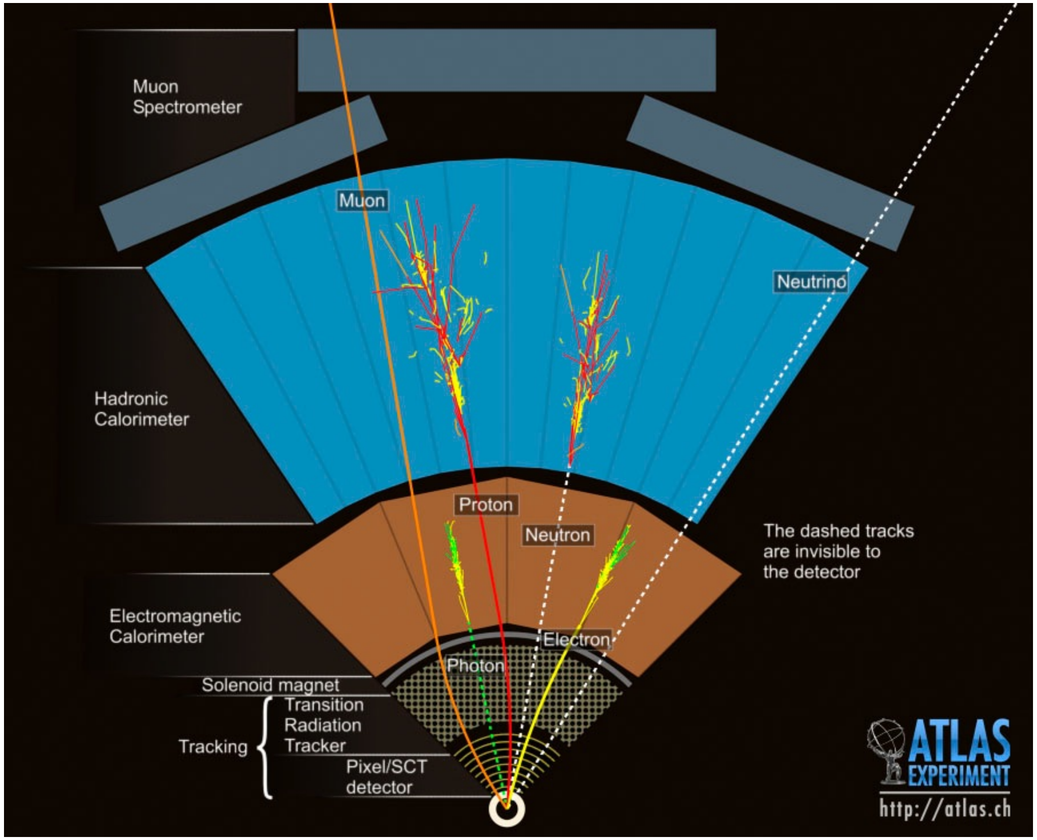

New for Run 2 @ ATLAS: Particle Flow

Alternative: "Particle Flow" approach

"Exploit full detector information to resolve, identify and measure each single particle!"

Photons (from π^0) measured in ECAL

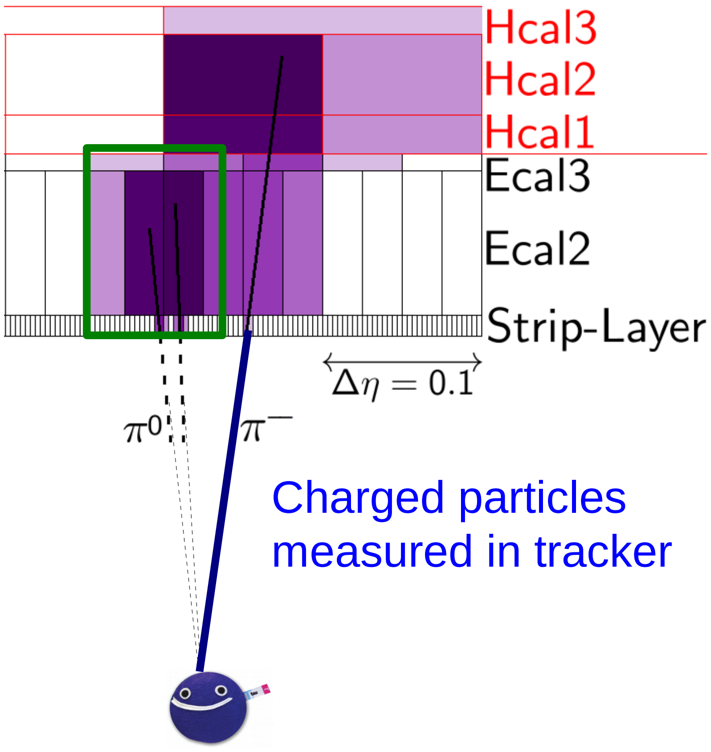

Charged particles measured in tracker

New for Run 2 @ ATLAS: Particle Flow

Alternative: “Particle Flow” approach

“Exploit full detector information to resolve, identify and measure each single particle!”

Photons (from π^0) measured in ECAL

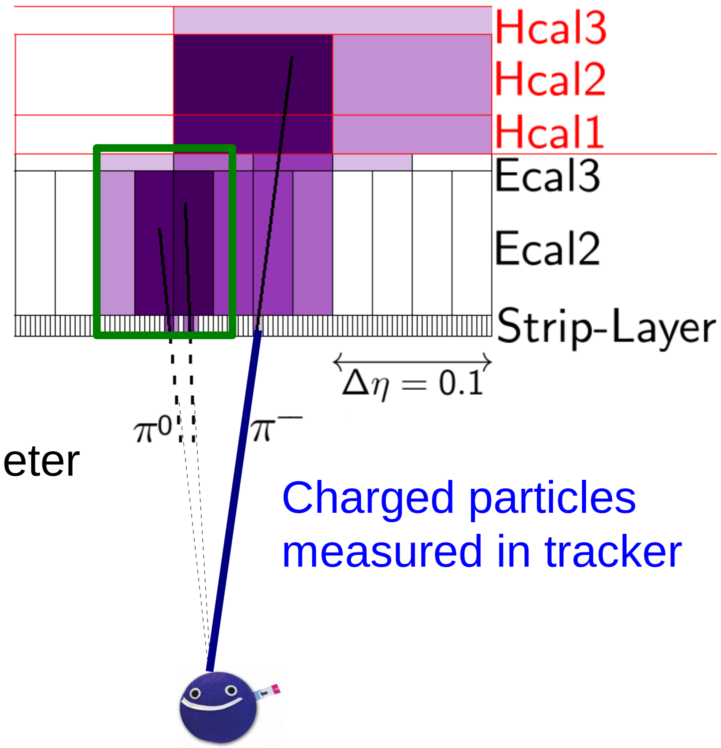

Challenge: Separate energy deposits in calorimeter from different particles (“confusion”)
→ Detector specifications important: granularity!

- Employed in various experiments to different extent – e.g. all Tevatron and LEP expmts.
- … and future: ILC detectors designed for Particle flow
- … and a contemporary: CMS – full event reconstruction with Particle Flow

Reconstruction Algorithm

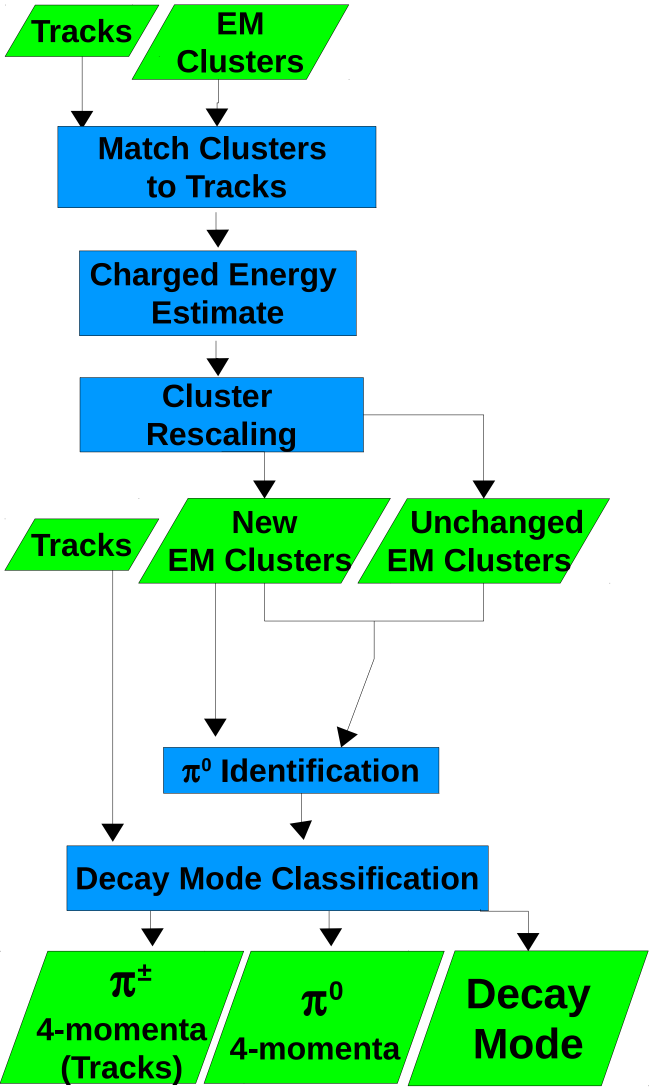

Reconstruction Algorithm

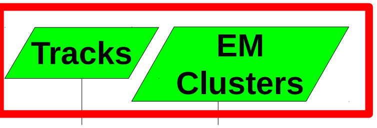

~99% of τ decays contain no neutral hadrons!

- Assign all HCAL energy → $\pi^{\pm}$
- redo clustering in EMCAL only

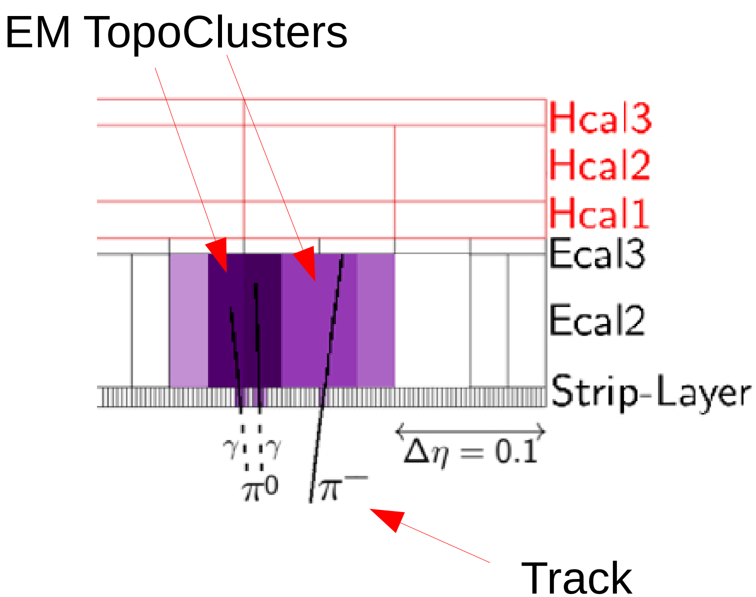

Reconstruction Algorithm

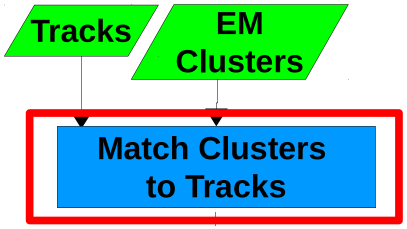

Match closest cluster to track

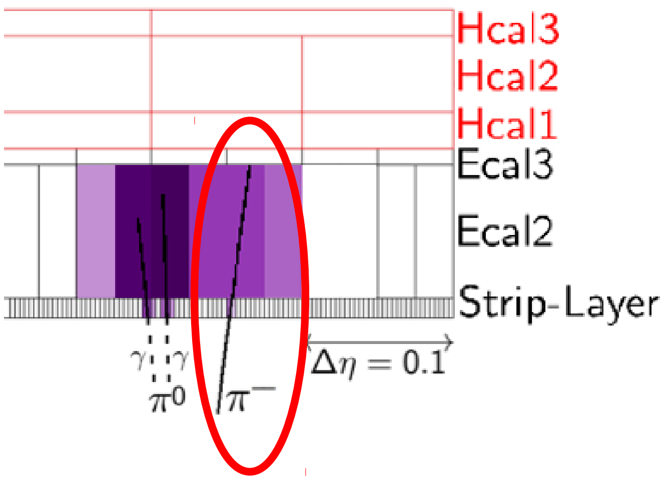

If no cluster found within 0.04 then assume $\pi^{\pm}$ did not leave a cluster → no subtraction

Reconstruction Algorithm

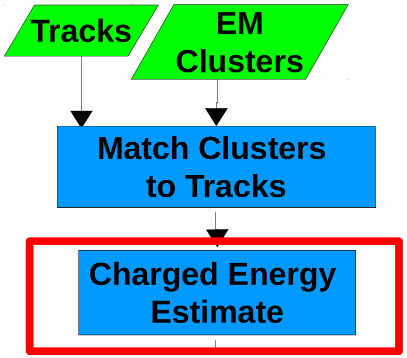

Estimate $\pi^{\pm}$ energy to be subtracted

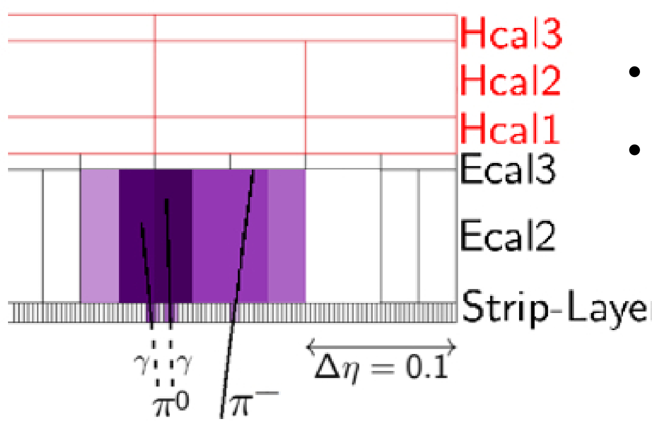

- Overlap of π^0 and $\pi^{\pm}$ only in ECAL
- Compute $\pi^{\pm}$ energy in ECAL simply as: $E_{exp}(\pi^{\pm})$ = p(track) – E(Hcal)

Reconstruction Algorithm

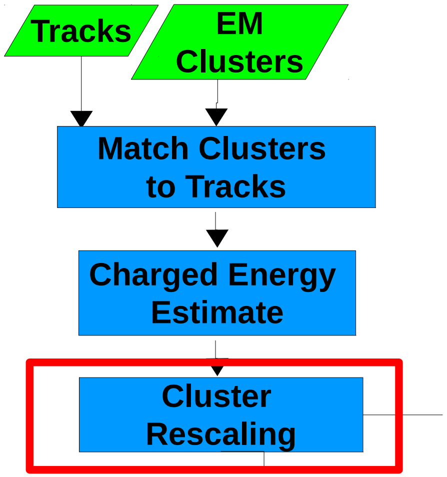

Subtract $E_{exp}(\pi^{\pm})$ from energy of matched cluster

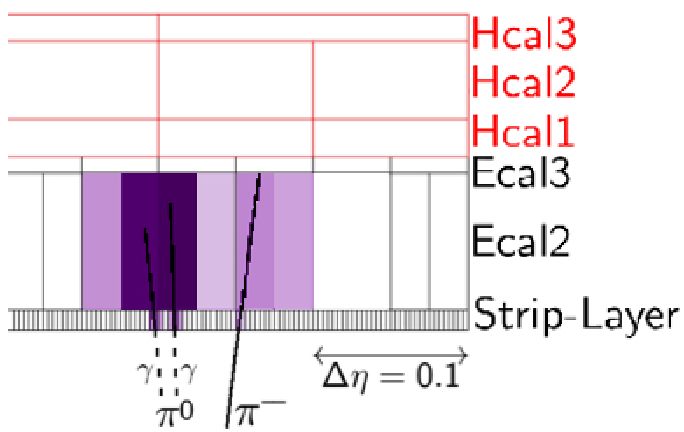

Reconstruction Algorithm

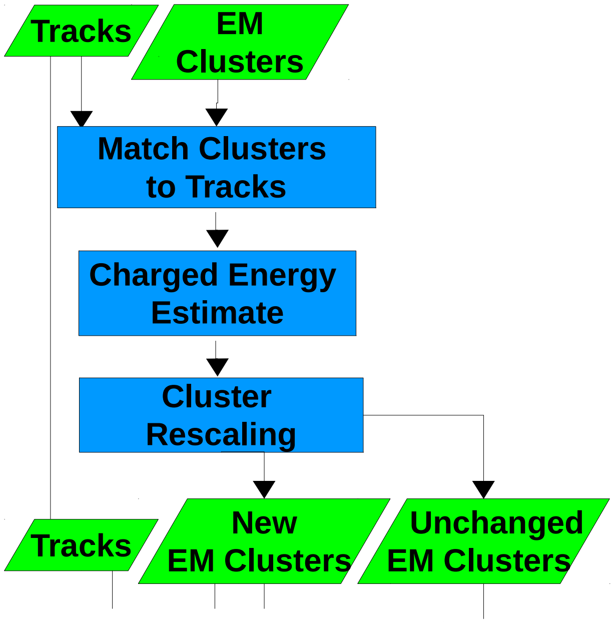

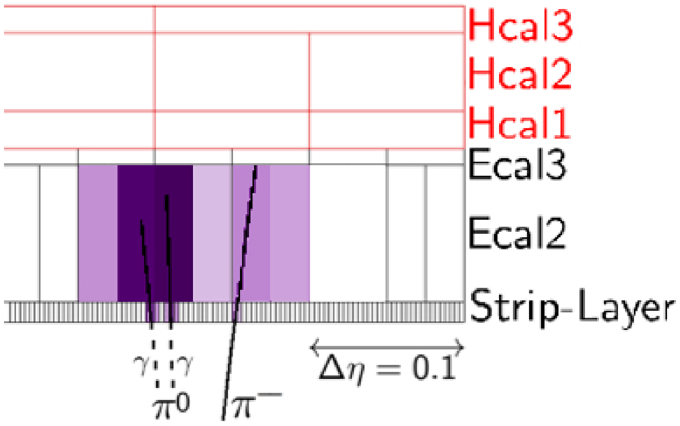

Reconstruction Algorithm

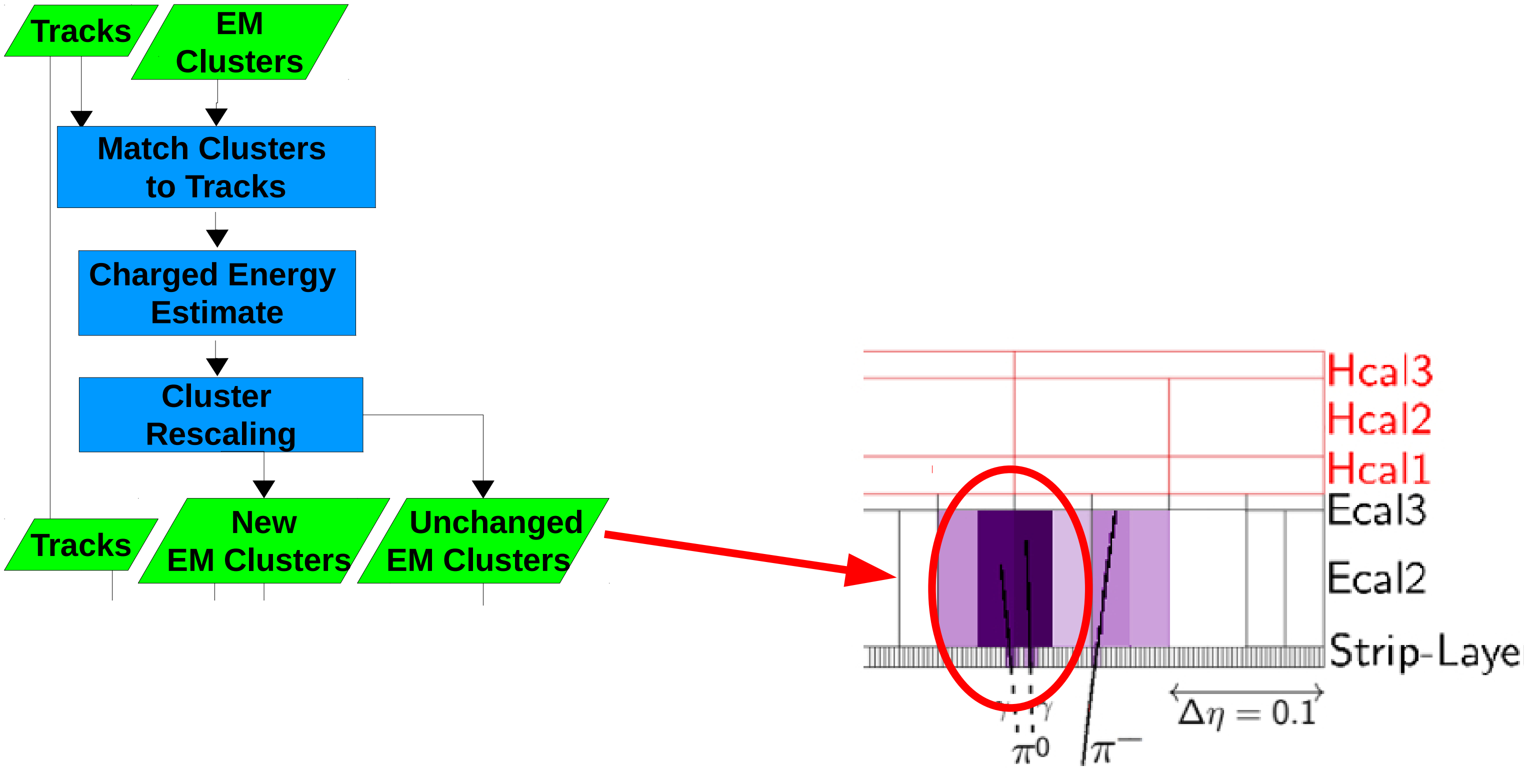

Reconstruction Algorithm

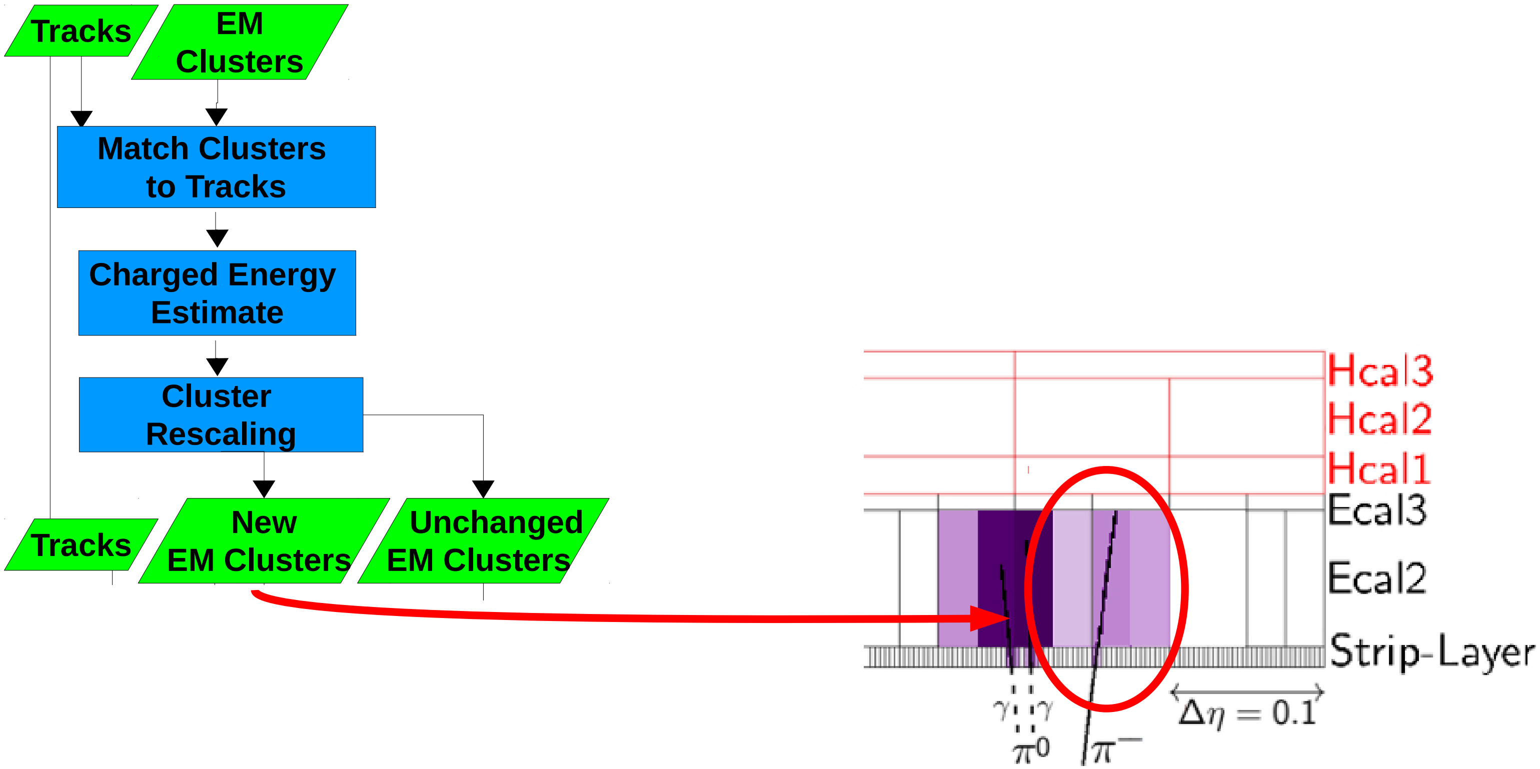

Reconstruction Algorithm

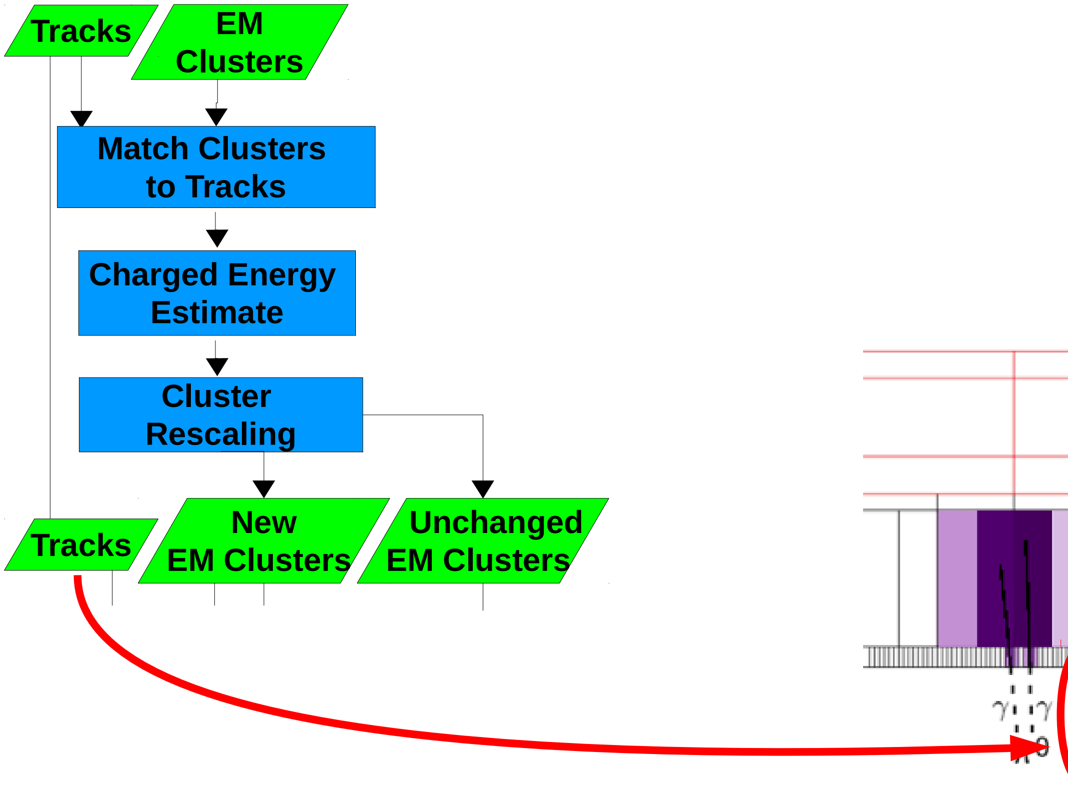

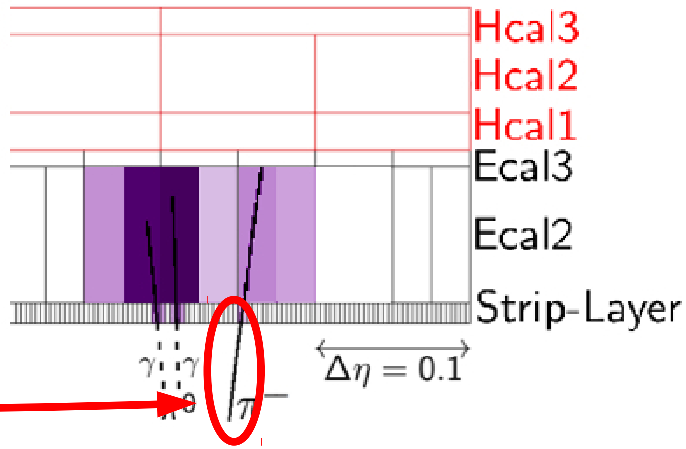

Reconstruction Algorithm

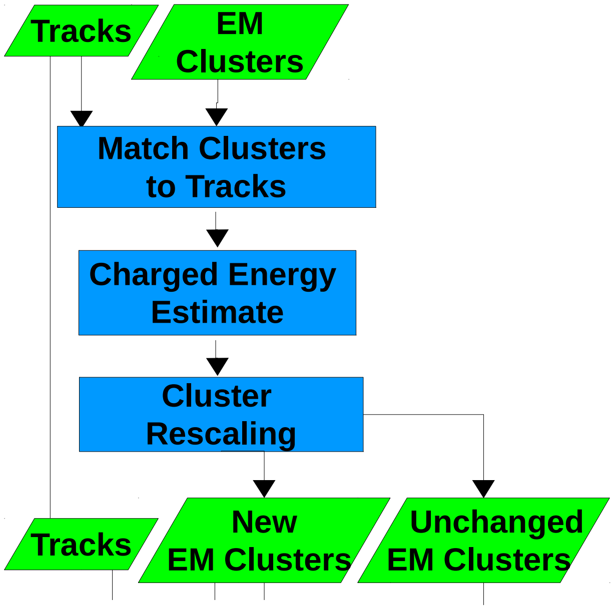

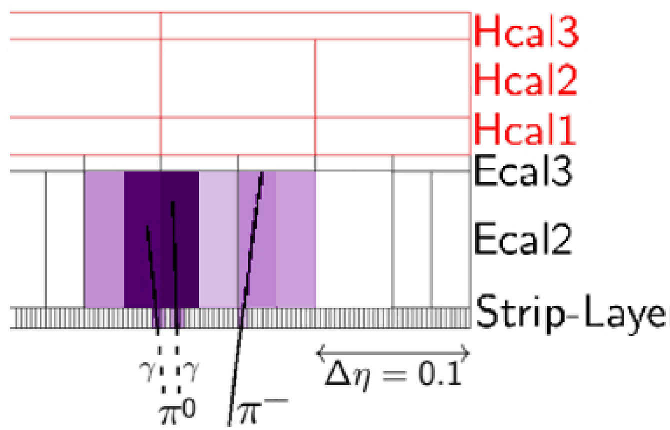

Instead of simply “throwing away” $\pi^{\pm}$ remnant cluster → significant performance gain by exploiting

- Cluster properties
- τ kinematics

Also: Important to pick the right π^0 cluster for analysis!

Reconstruction Algorithm

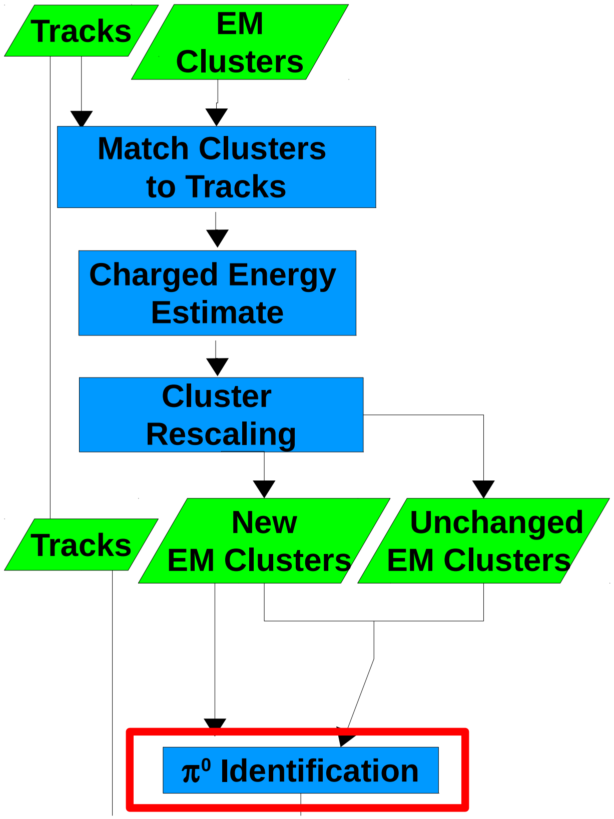

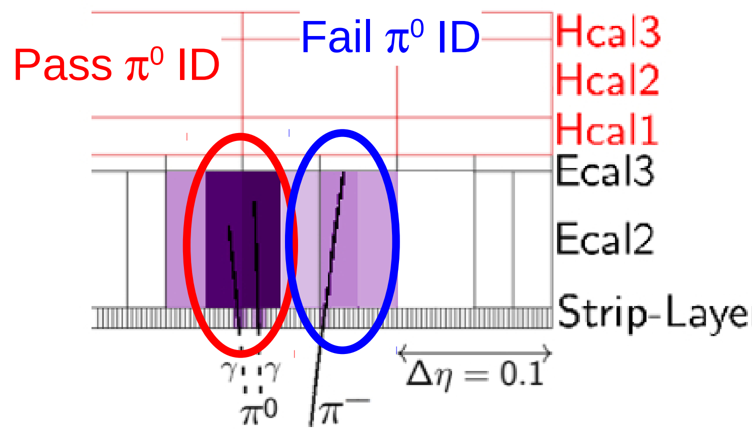

Suppress $\pi^{\pm}$ remnants using BDT based on

- Cluster moments
- Number of photons

Reconstruction Algorithm

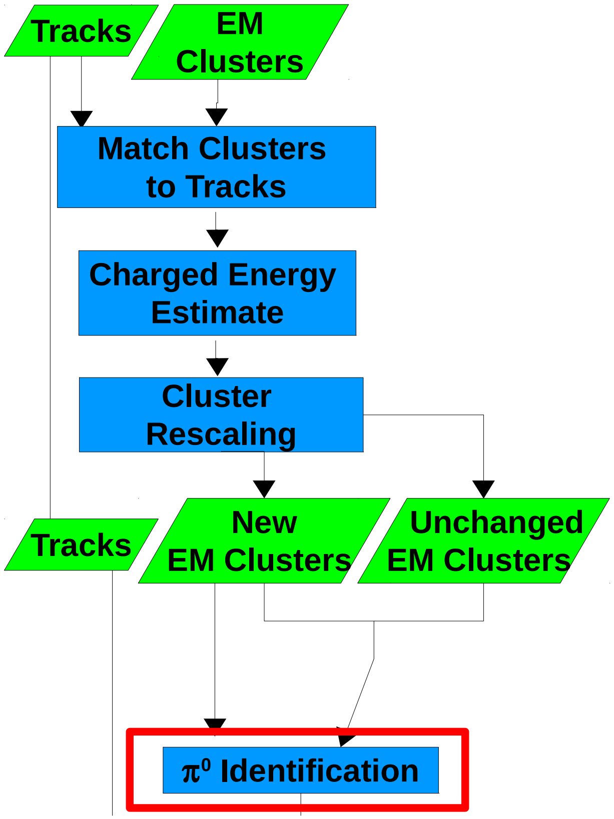

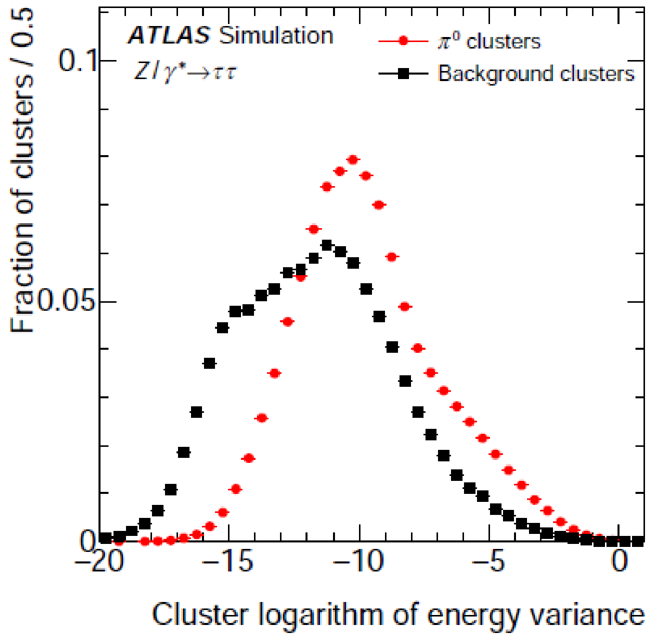

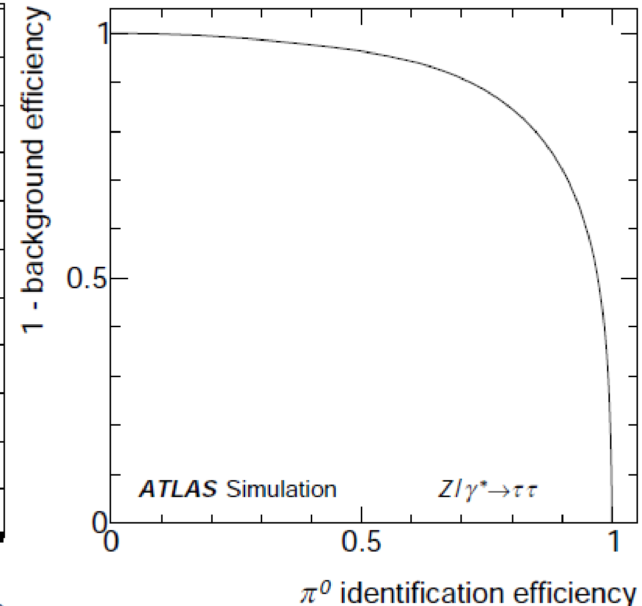

Suppress $\pi^{\pm}$ remnants using BDT based on

- Cluster moments
- Number of photons

Reconstruction Algorithm

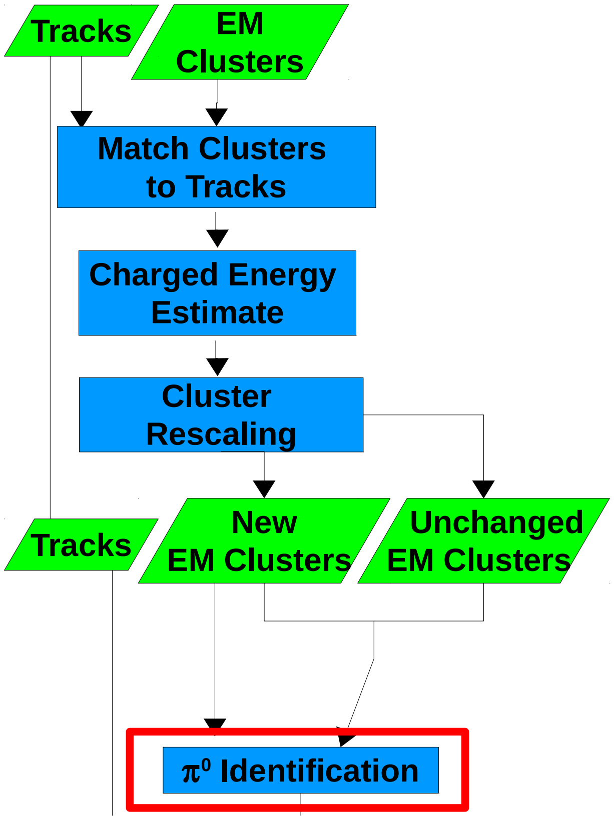

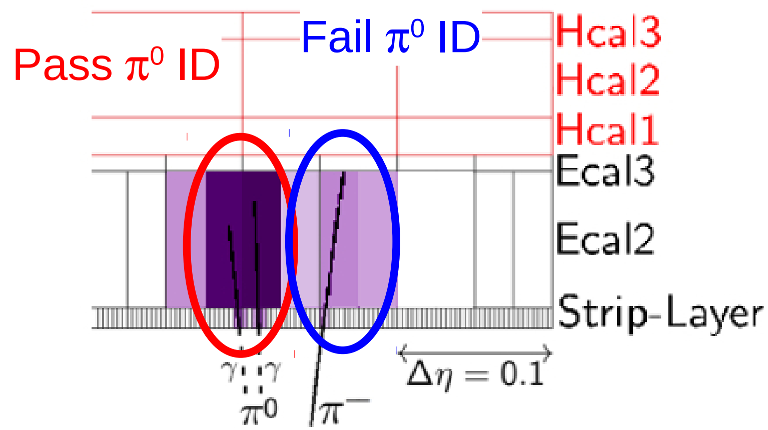

Suppress $\pi^{\pm}$ remnants using BDT based on

- Cluster moments
- Number of photons

→ This in combination with a cut on E_T(neutral) > ~2 GeV gives the gain in particle flow τ resolution!

Reconstruction Algorithm

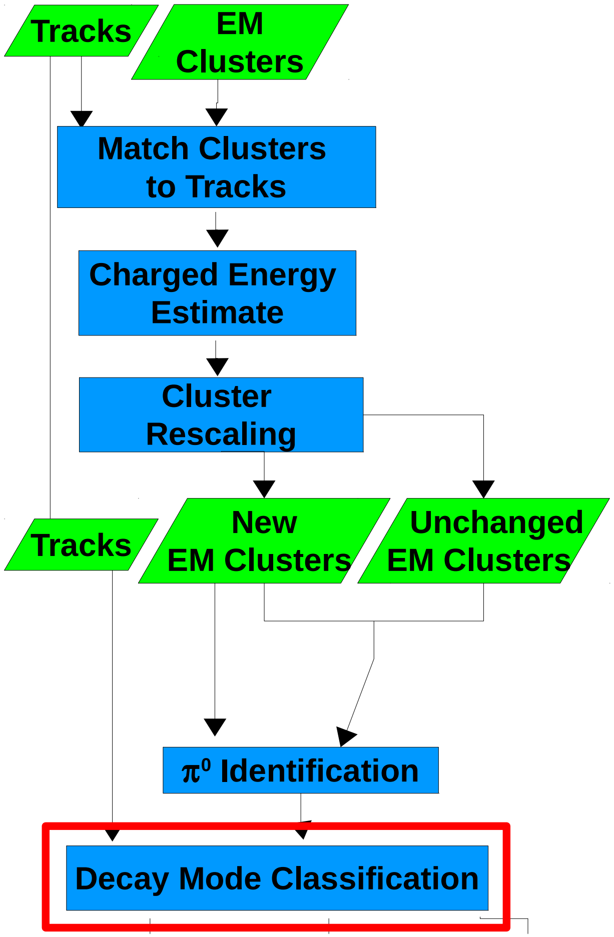

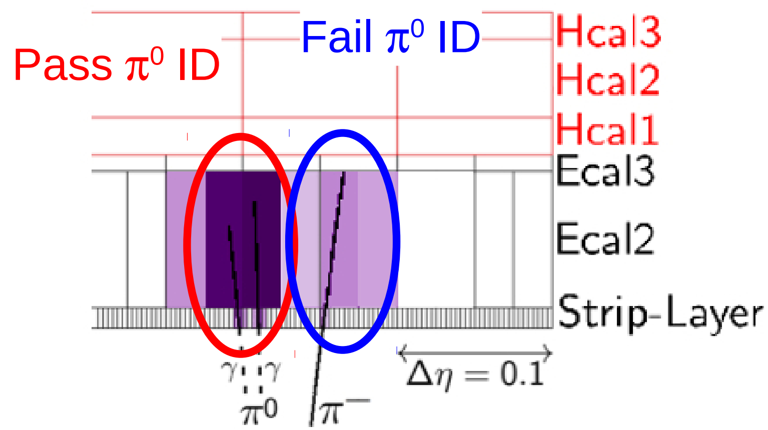

Classify decay mode using

- Decay kinematics
- π^0 ID information
- Number of photons

Reconstruction Algorithm

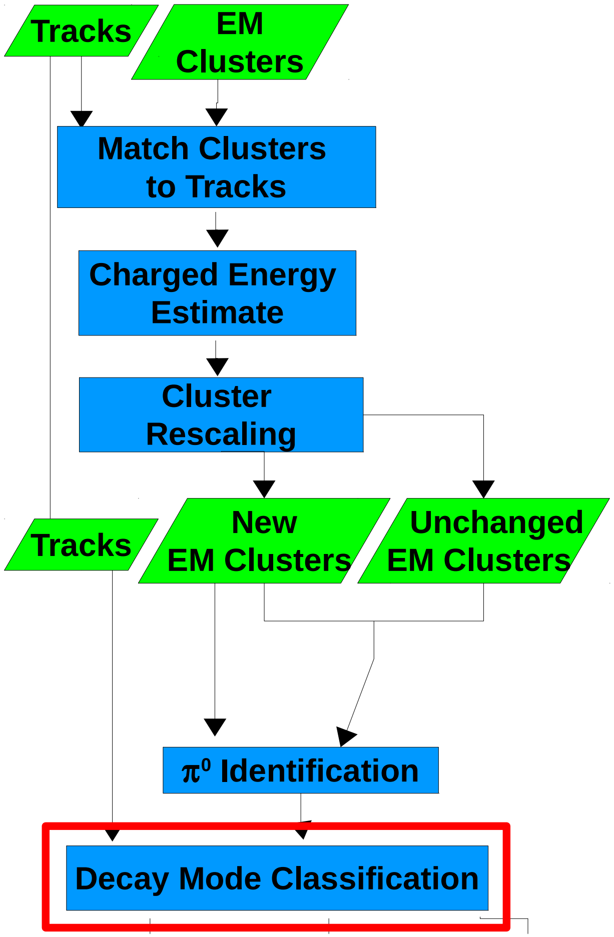

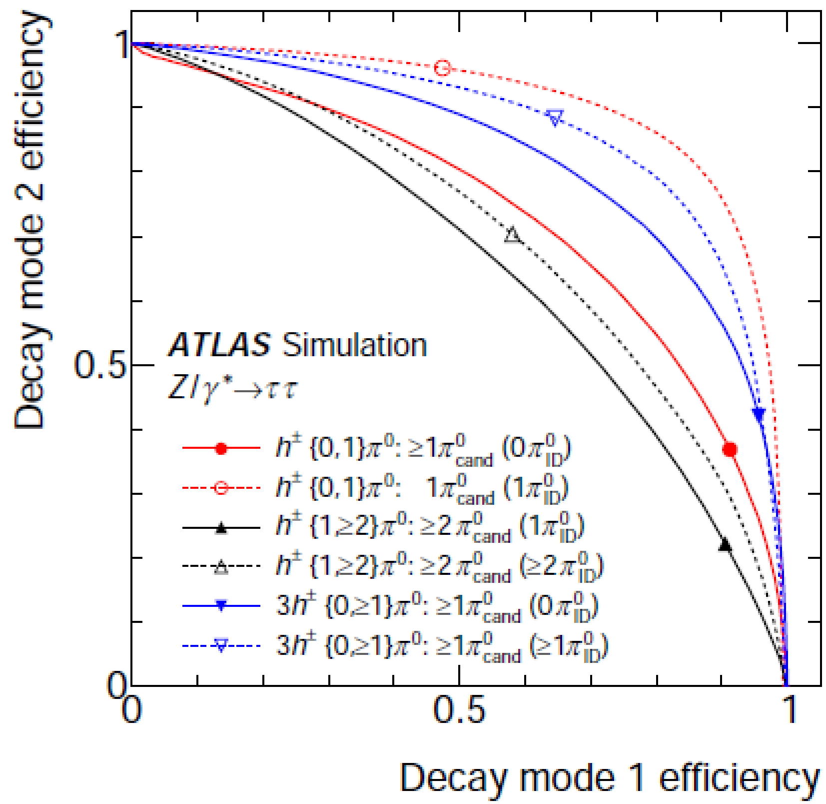

Classify decay mode using

- Decay kinematics
- π^0 ID information
- Number of photons

Reconstruction Algorithm

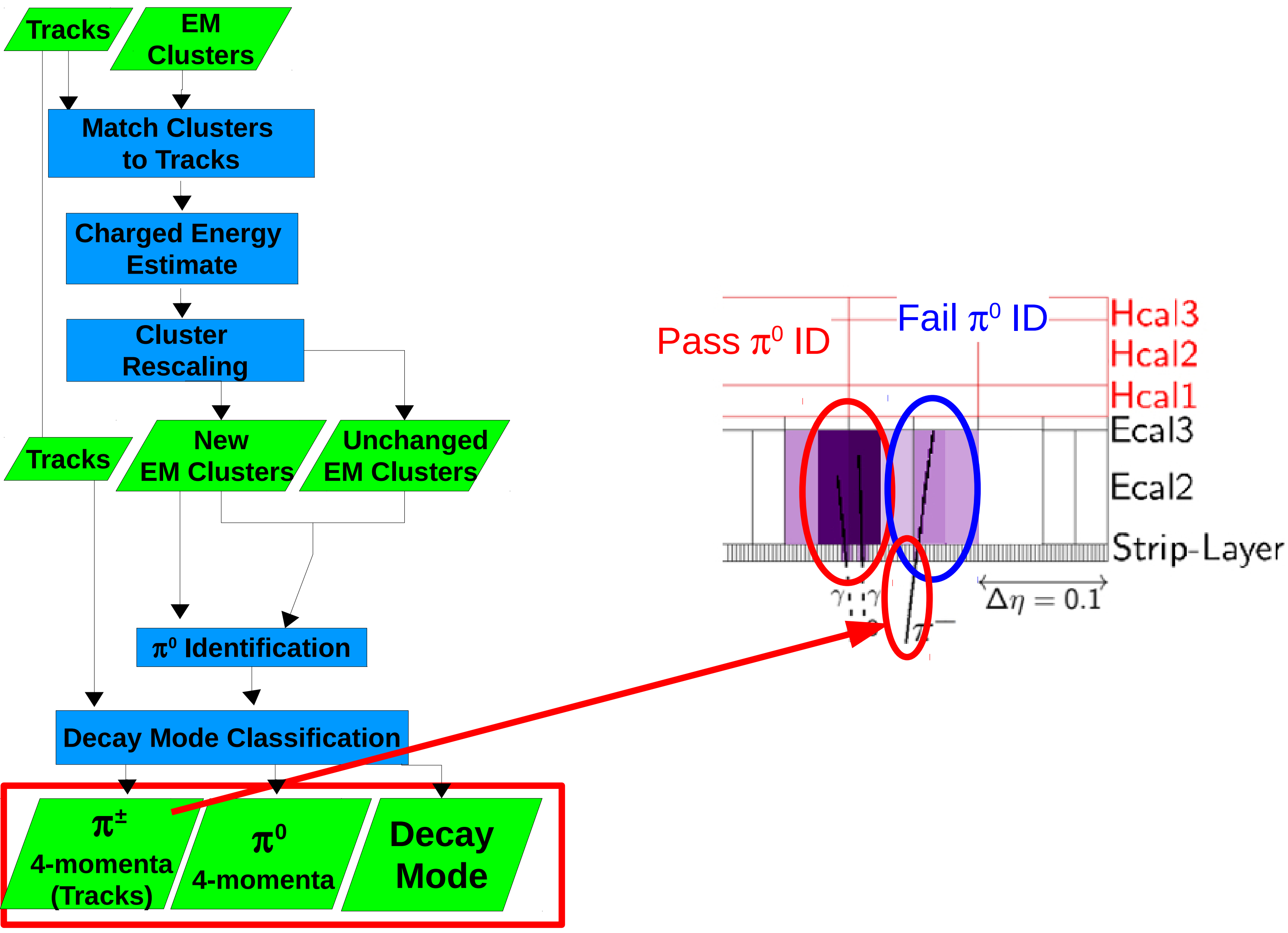

Reconstruction Algorithm

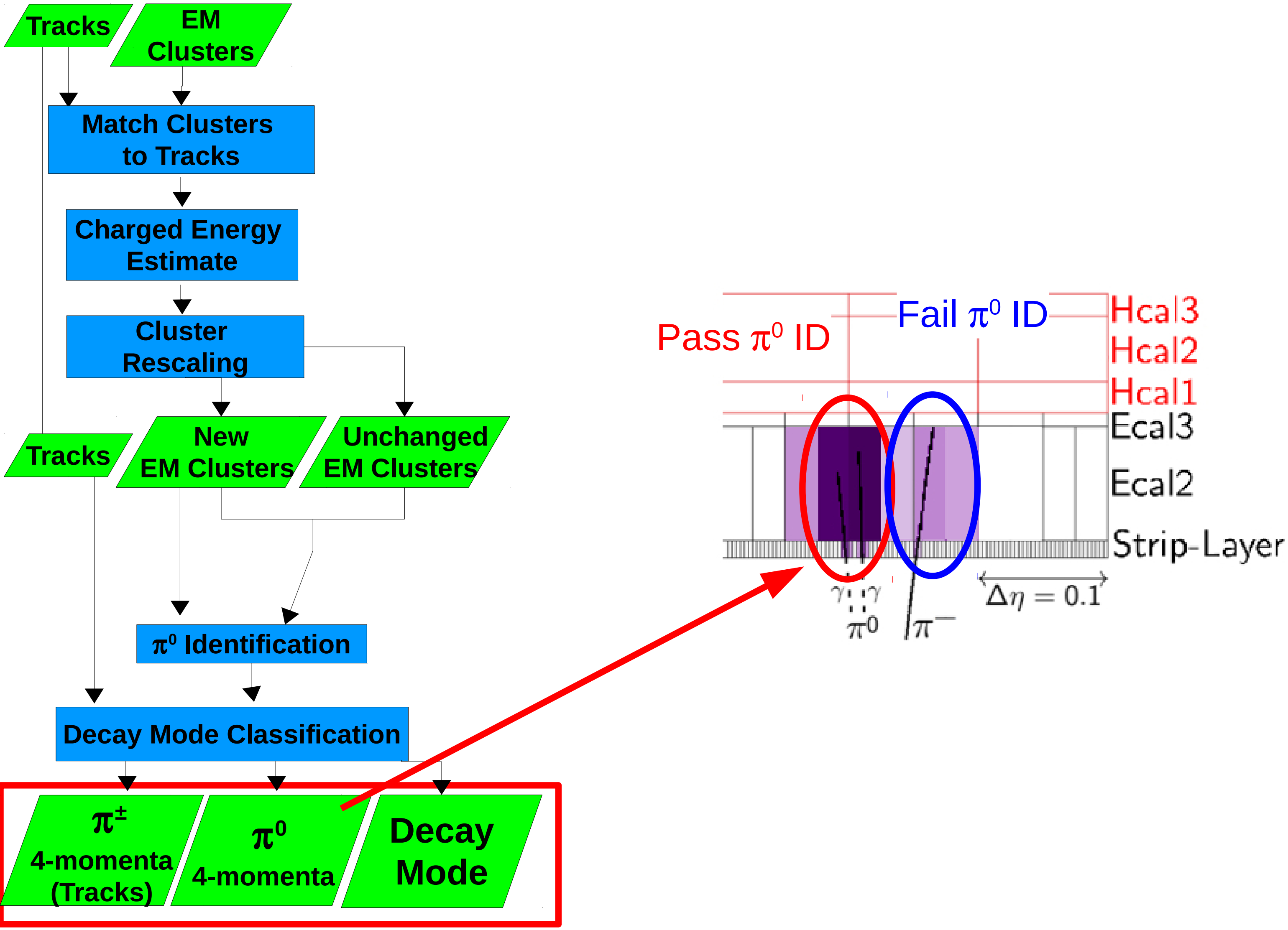

Reconstruction Algorithm

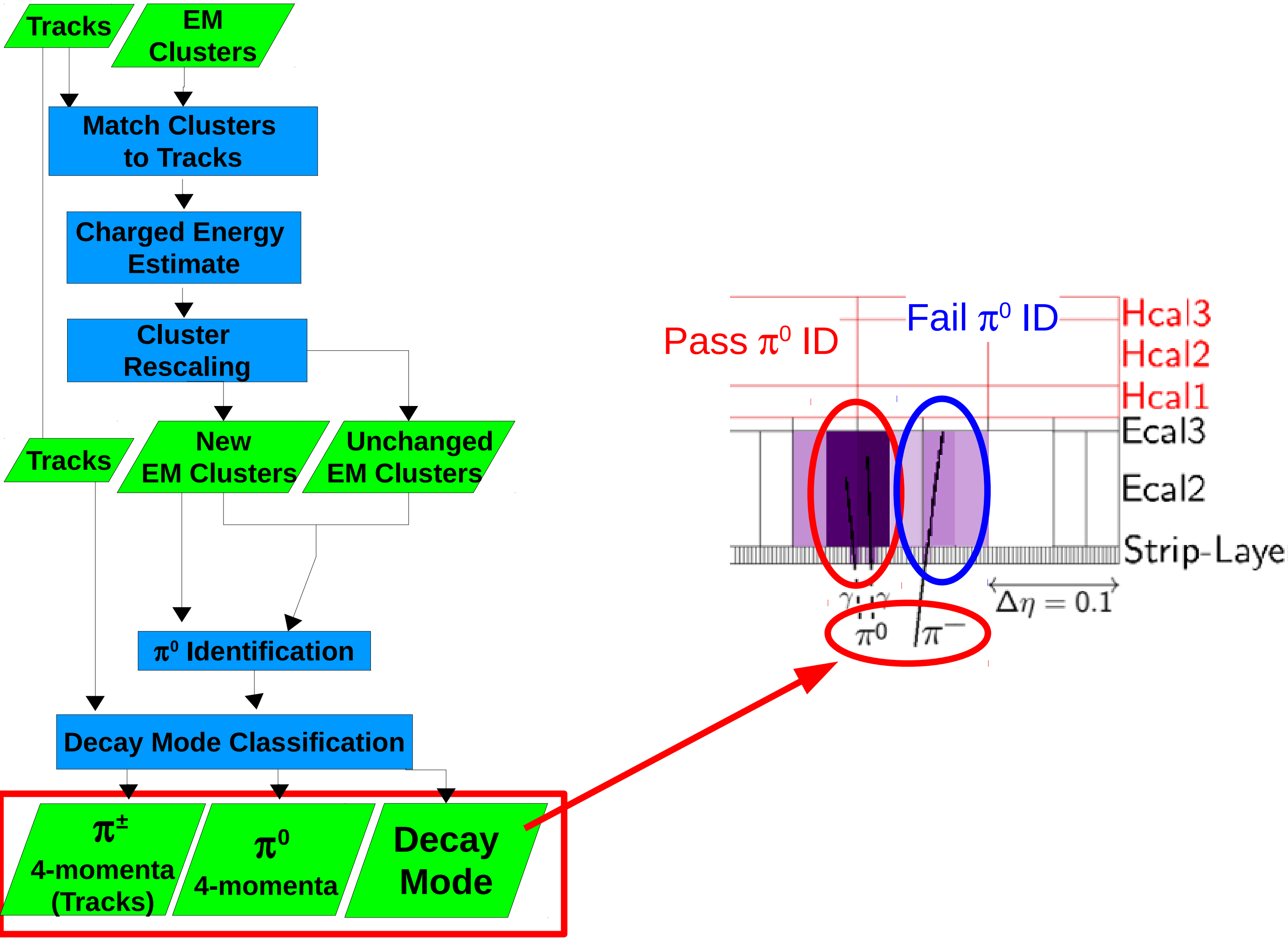

Reconstruction Algorithm

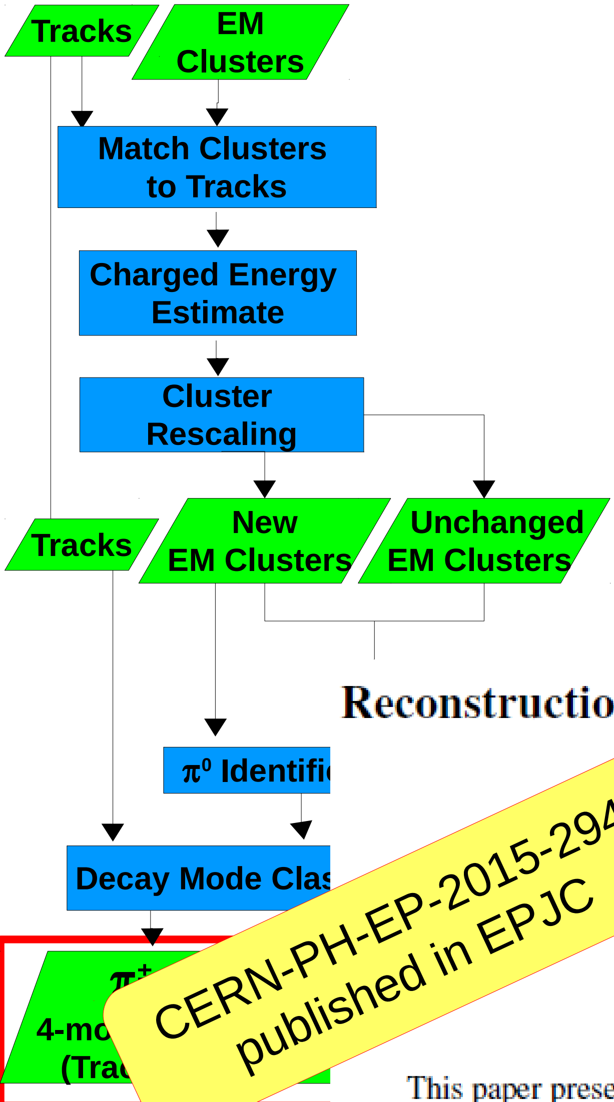

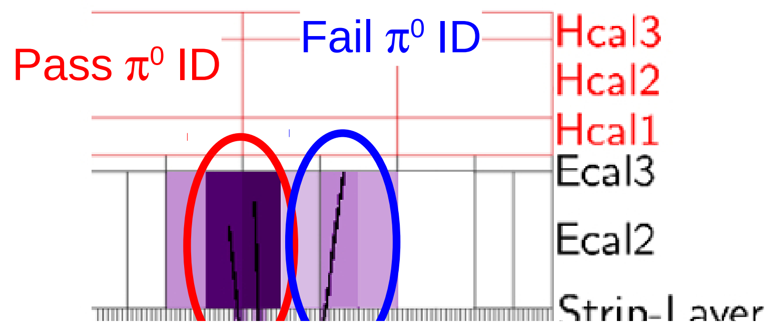

CERN-PH-EP-2015-294
published in EPJC

Reconstruction of hadronic decay products of tau leptons with the ATLAS experiment

The ATLAS Collaboration

Abstract

This paper presents a new method of reconstructing the individual charged and neutral hadrons in tau decays with the ATLAS detector. The reconstructed hadrons are used to classify the decay mode and to calculate the visible four-momentum of reconstructed tau candidates, significantly improving the resolution with respect to the calibration in the existing tau re-

Particle flow performance – What do we gain?

What's the gain? – 4-vector resolution

Better 4-momentum resolution than calorimeter-only in Run 1:

- Angular resolution: >5 times improved

CERN-PH-EP-2015-294

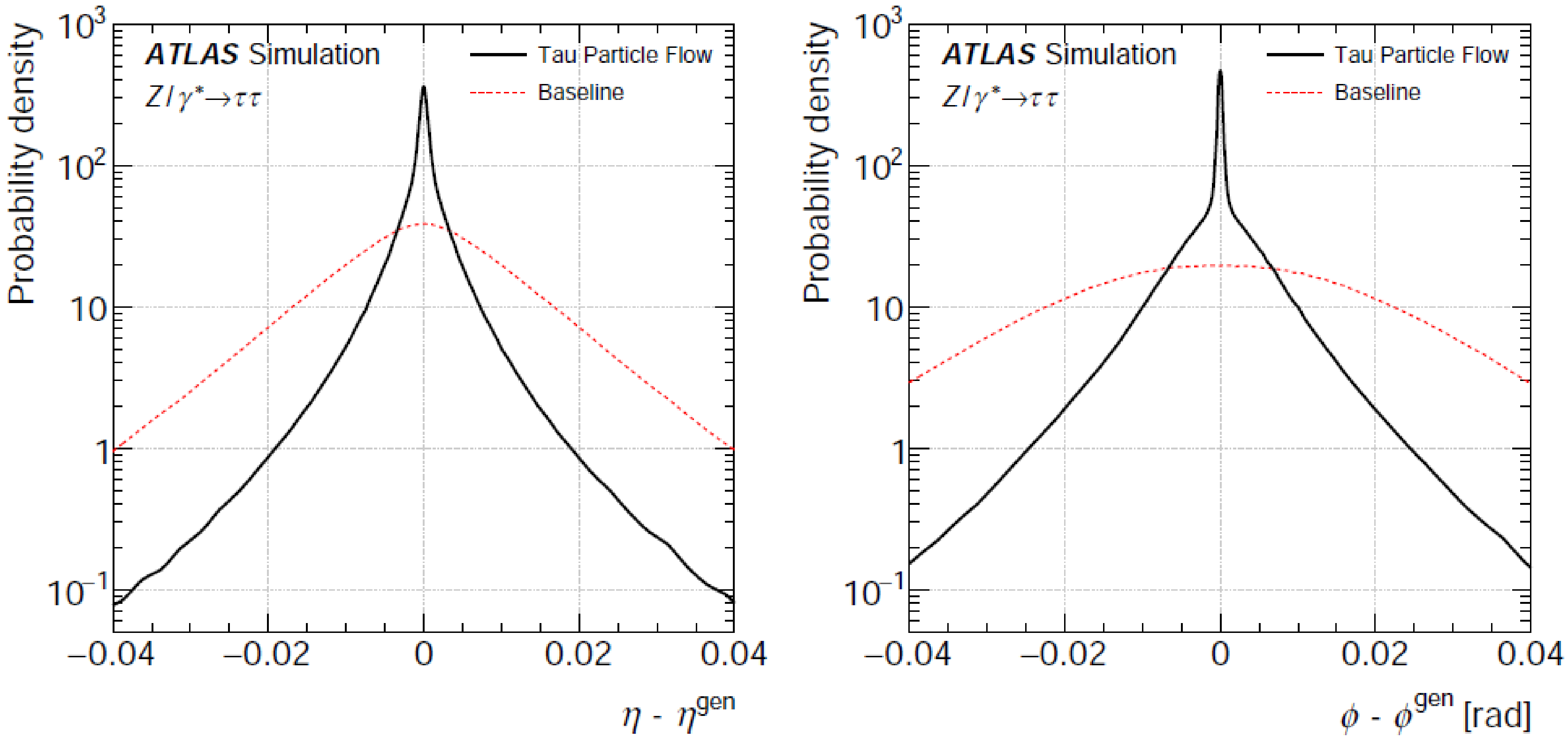

What's the gain? – 4-vector resolution

Better 4-momentum resolution than calorimeter-only in Run 1:

- Angular resolution: >5 times improved
- Energy resolution: ~2 times improved at low E_T

CERN-PH-EP-2015-294

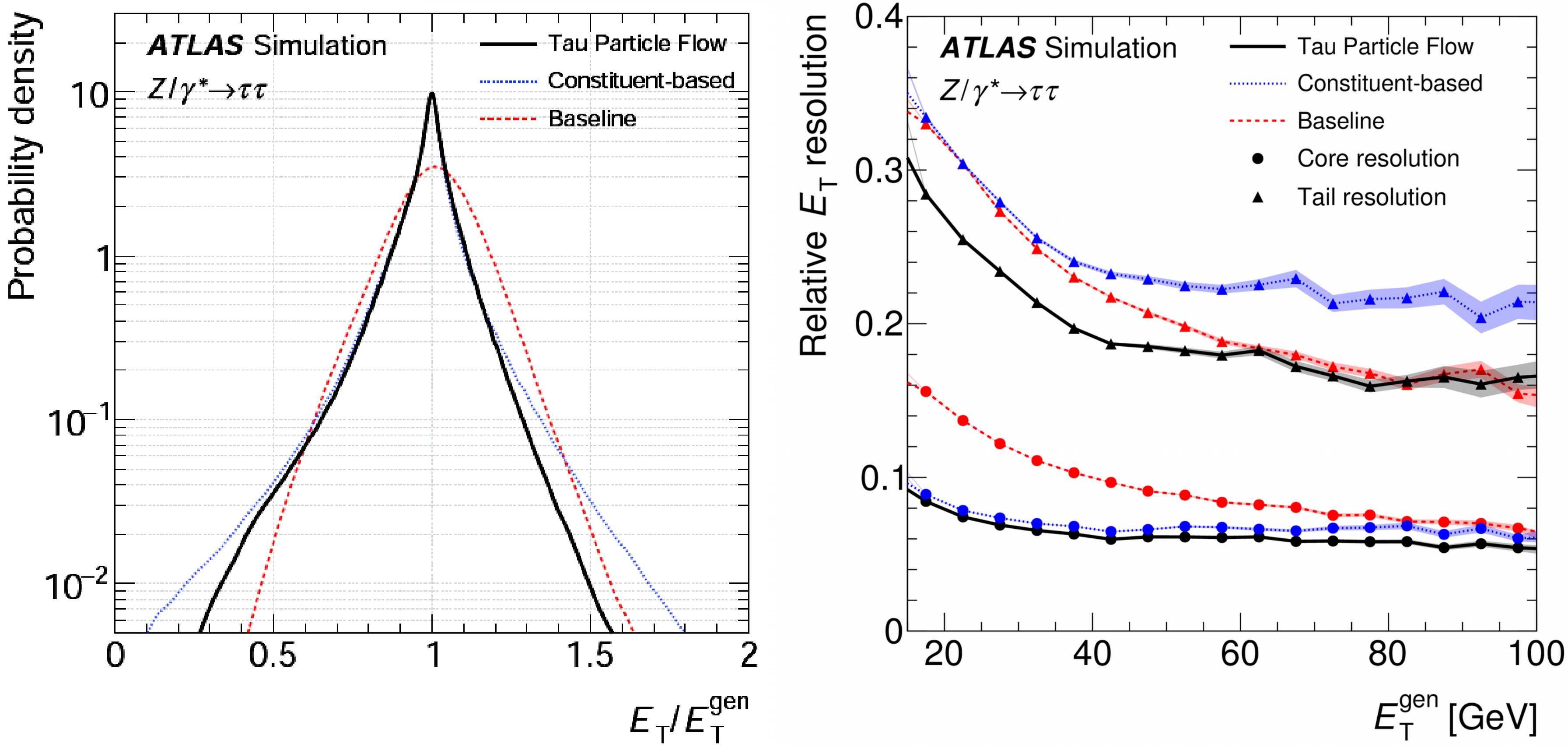

What's the gain? – 4-vector resolution

CERN-PH-EP-2015-294

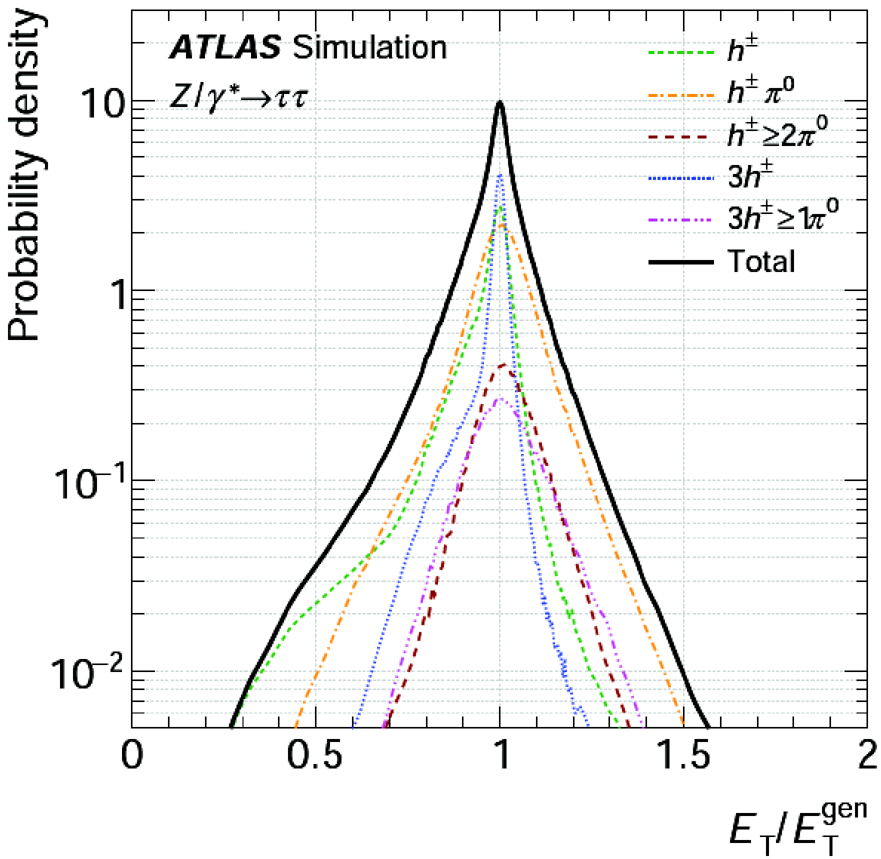

Features of resolution distribution:

- Best resolution for modes without $\pi^{\pm}$ and correctly reconstructed decays
- Misestimation of π^0 → bias of ~25%
- Large low-energy bias from decays with neutral Kaons (not fully reconstructed)

What's the gain? – 4-vector resolution

Better 4-momentum resolution than calorimeter-only in Run 1:

- Angular resolution: >5 times improved
- Energy resolution: ~2 times improved at low E_T
- Performance quite insensitive to busy-ness of collision environment

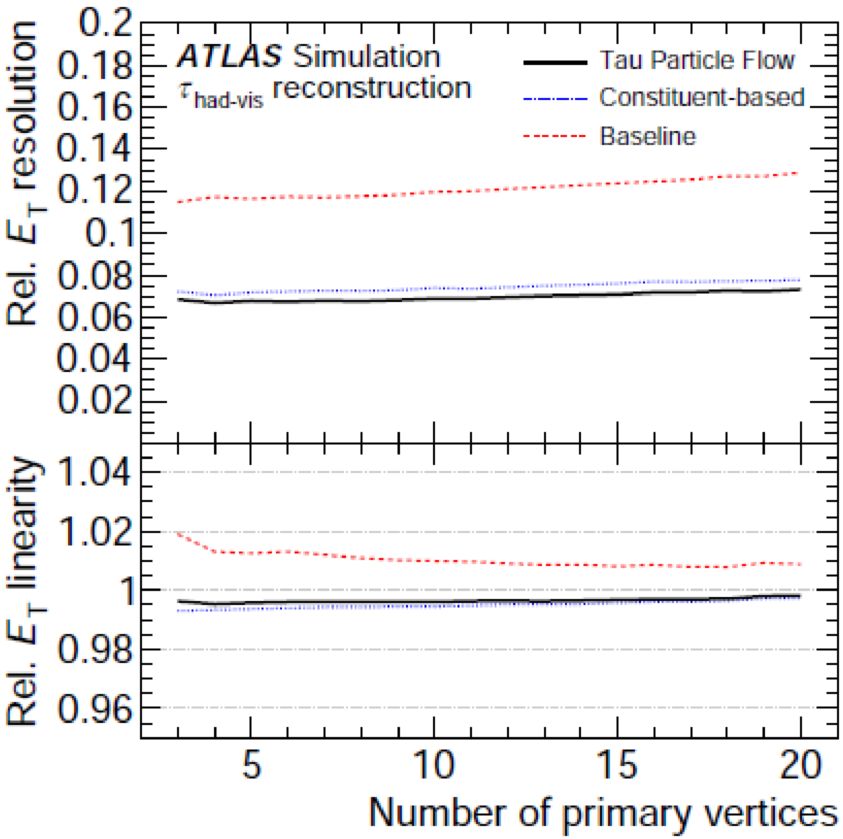

CERN-PH-EP-2015-294

("Offset" correction of ~100-400 MeV applied to Run 1 here)

What's the gain? – 4-vector resolution

Better 4-momentum resolution than calorimeter-only in Run 1:

- Angular resolution: >5 times improved
- Energy resolution: ~2 times improved at low E_T
- Performance quite insensitive to busy-ness of collision environment
- Performance also well modeled in data!

CERN-PH-EP-2015-294

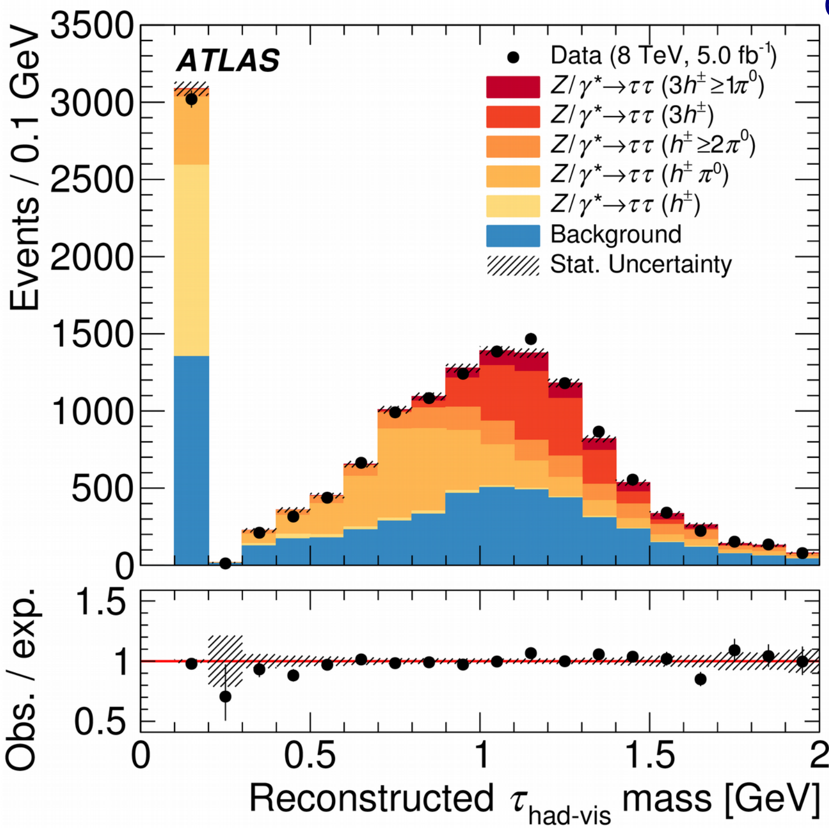

Same plot also on the EPJC cover!

Particle Flow – What does it give us beyond a better 4-momentum measurement?

What's the gain? – H vs. Z discrimination

$Z \rightarrow \tau\tau$ major background in $H \rightarrow \tau\tau$ analysis

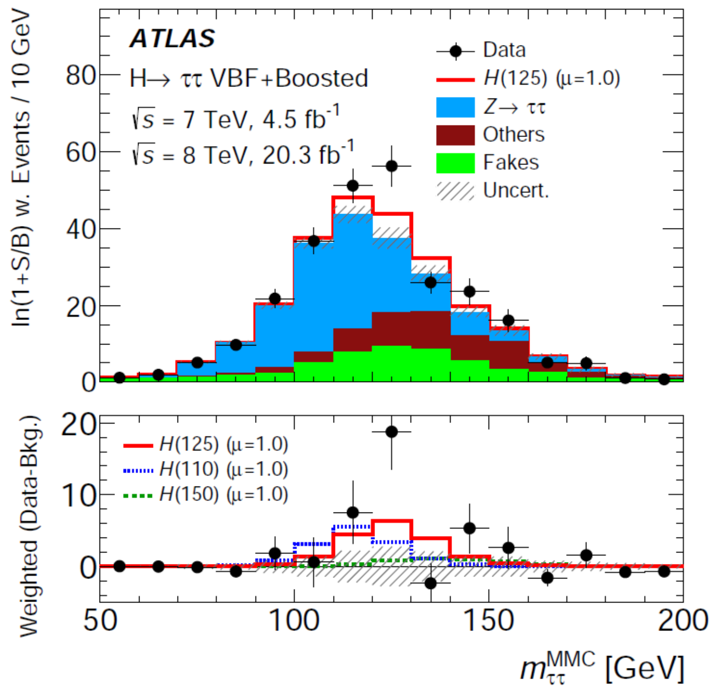

Yet unexploited: Discriminate Z (vector) from H (scalar) using longitudinal τ polarization

What's the gain? – H vs. Z discrimination

Discriminate

Z (vector)

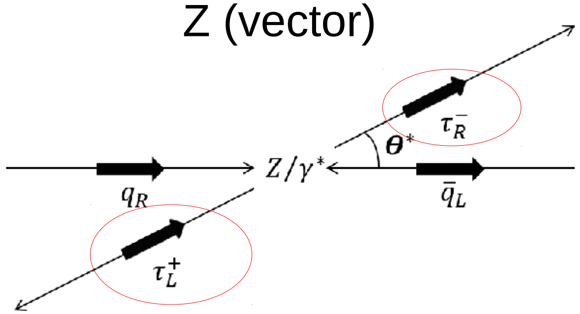

H (scalar)

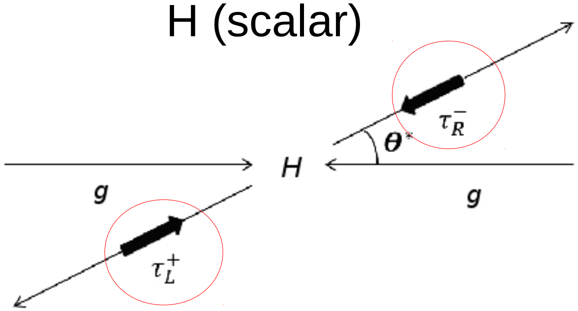

Longitudinal τ polarization

anti-correlated

correlated

What's the gain? – H vs. Z discrimination

Discriminate

Z (vector)

H (scalar)

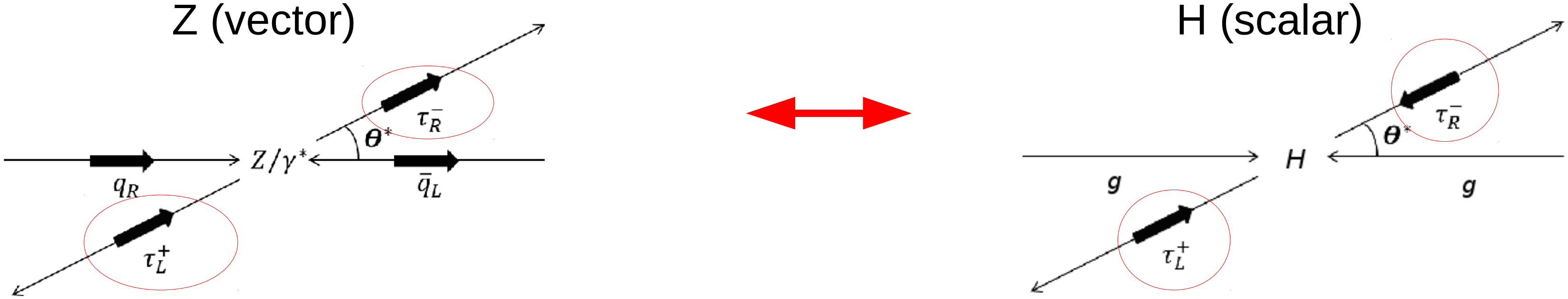

Longitudinal τ polarization

Measured in each τ using energy asymmetry of π and π^0 in $\tau \rightarrow \pi\pi^0\nu$ decays

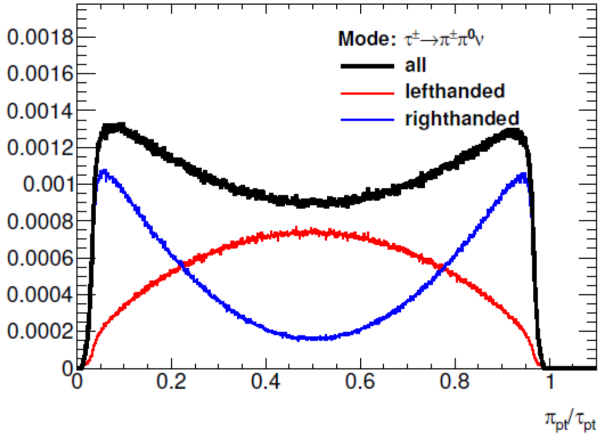

Prospects for Higgs CP Measurement

NEW

H → ττ important:

• Pseudoscalar Higgs in major models does not couple at tree level to WW and ZZ → need fermionic final states!

• Tau is only lepton that gives access to polarization through kinematics of its decay products → need Particle Flow!

→ Higgs CP measurement in its decay by correlating **transverse** τ polarizations

Prospects for Higgs CP Measurement

Higgs CP measurement by correlating **transverse** τ polarizations:

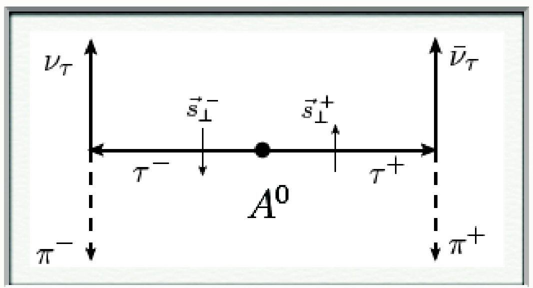

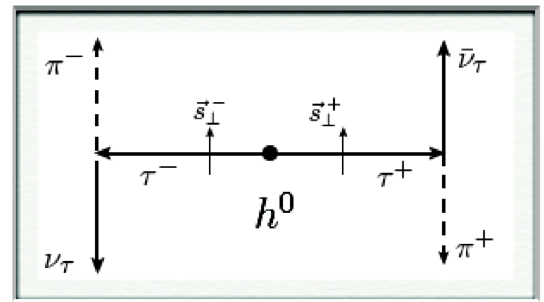

π^+ and π^- preferably parallel

π^+ and π^- preferably antiparallel

Measured using angle between τ decay planes:

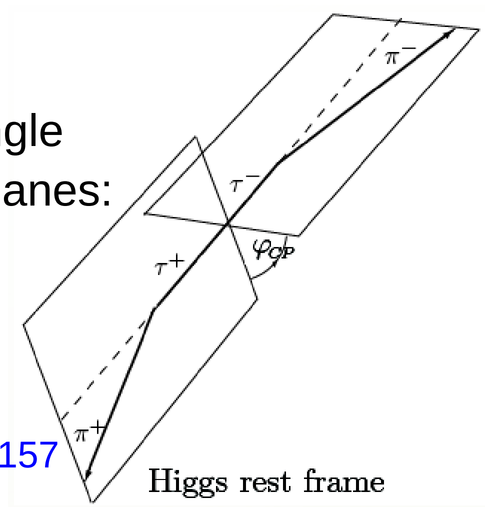

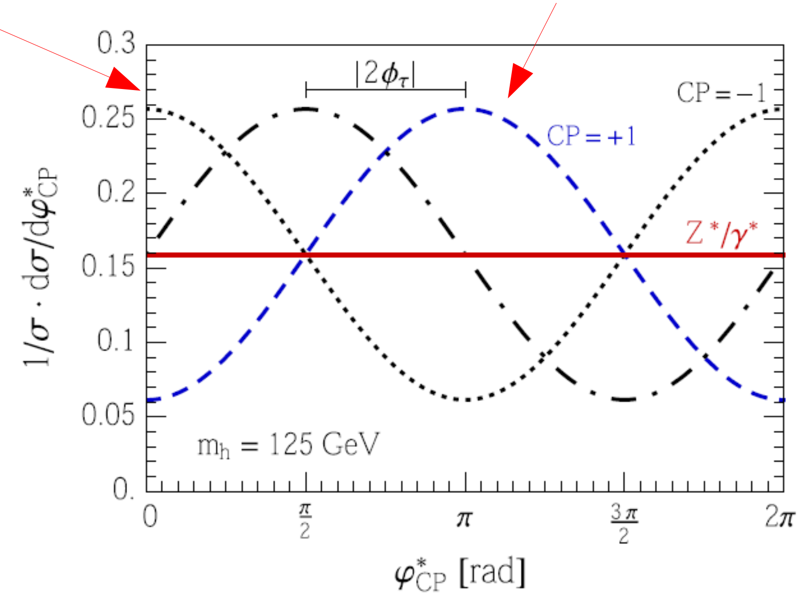

Desch et al,
Phys. Lett. B 579 (2004) 157
Berge et al,
Eur. Phys. J. C 74 (2014) 3164

Prospects for Higgs CP Measurement

Higgs CP measurement by correlating **transverse** τ polarizations:

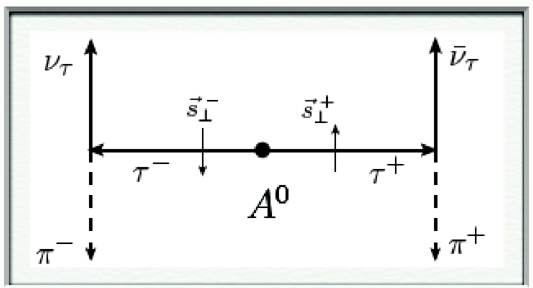

π^+ and π^- preferably parallel

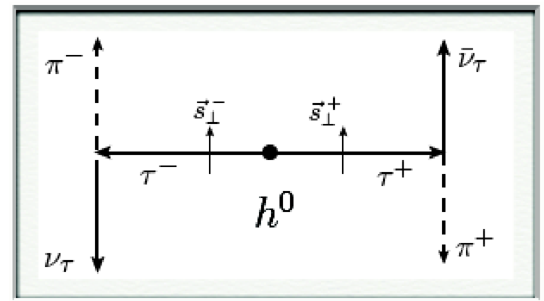

π^+ and π^- preferably antiparallel

Measured using angle between τ decay planes:

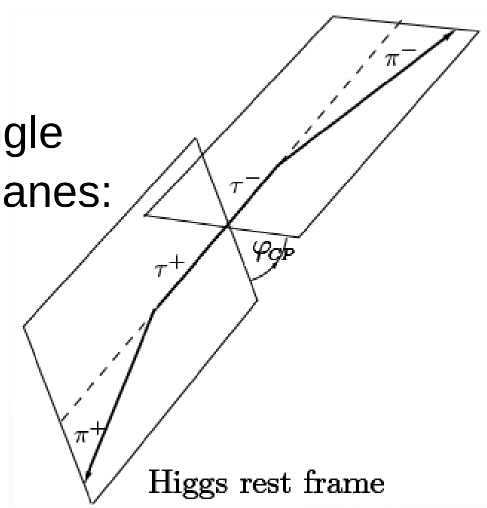

Actual reconstruction of decay planes dependent on decay mode!

Particle Flow Performance for CP Meas.

Five-way decay mode classification:
74.7% efficiency

Can resolve single π^0:
Energy core resolution 16%

Efficiency:

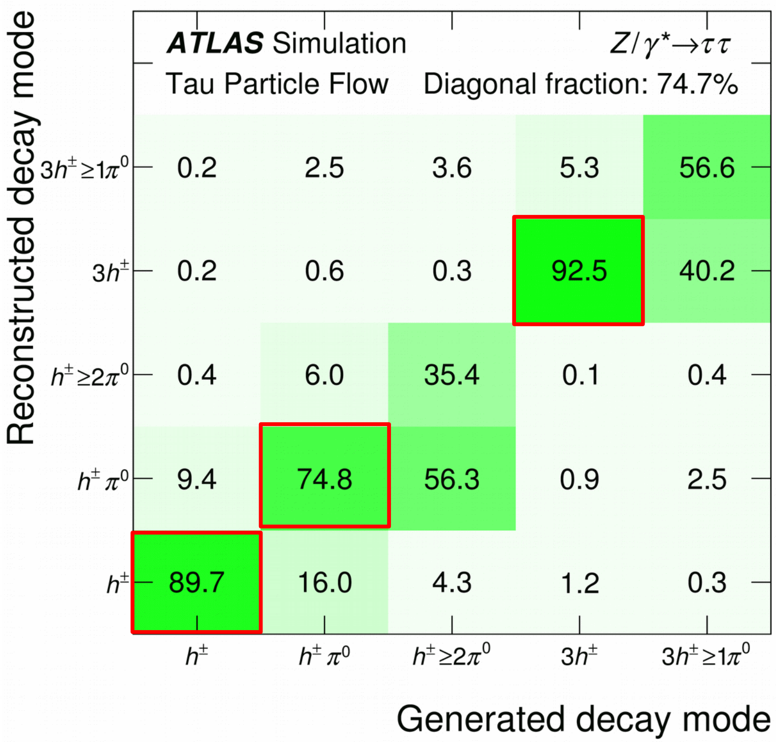

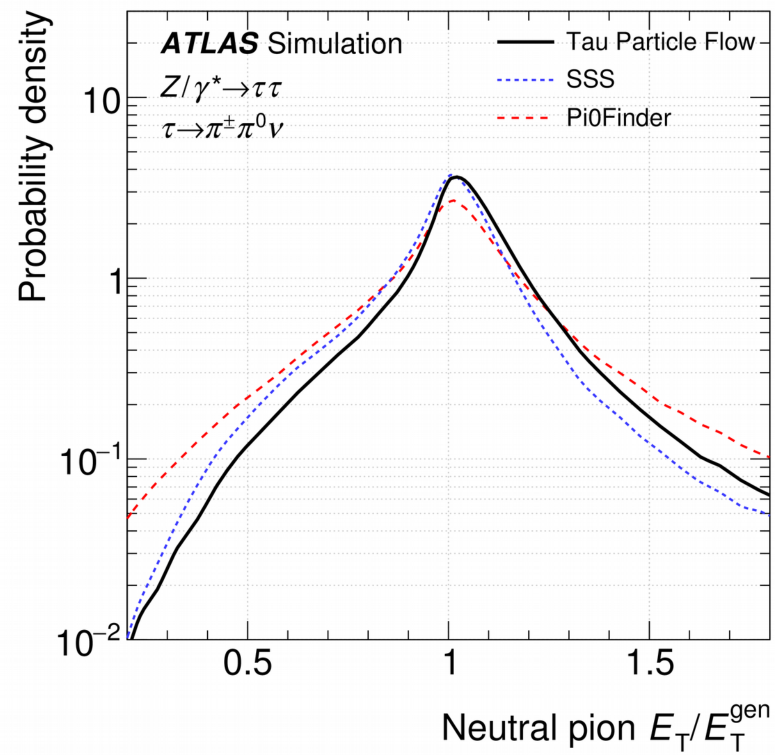

→ This makes CP state measurement in H → ττ possible!

CERN-PH-EP-2015-294

Particle Flow Performance for CP Meas.

NEW

Five-way decay mode classification:
74.7% efficiency

Well modeled:

CERN-PH-EP-2015-294

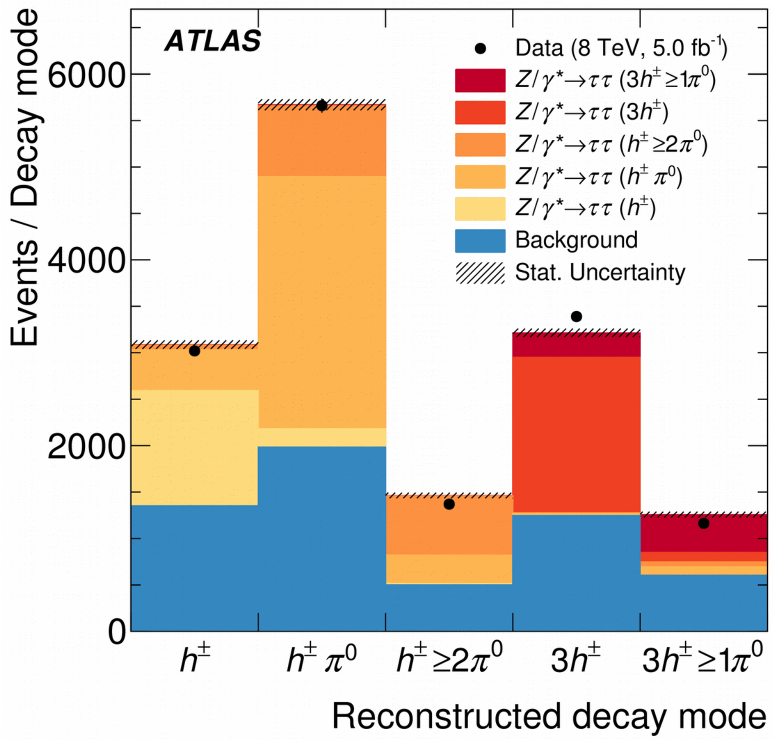

→ This makes CP state measurement in $H \to \tau\tau$ possible!

Conclusions

- Particle flow reconstruction for tau leptons is being prepared for ATLAS analysis
- Tau reconstruction benefits significantly from Particle flow

- 5-way decay-mode classification → Higgs CP
- E_T core resolution of τ_{vis} improved by factor ~2 at low E_T
- Angular resolution improved by factor ~5

Backup


http://www.DigitalLaughter.com
MY COMPUTER DOESN'T WORK! THE HARD DRIVE CRASHED! WHAT DO I DO?!
DID YOU BACK UP?
WHY? IS IT GONNA BLOW?!

Important Physics Results with τ's

H → ττ evidence

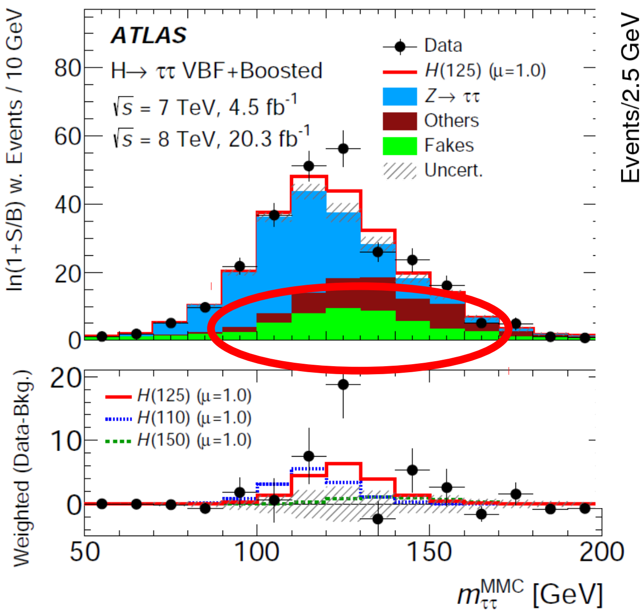

SM Z → ττ cross section

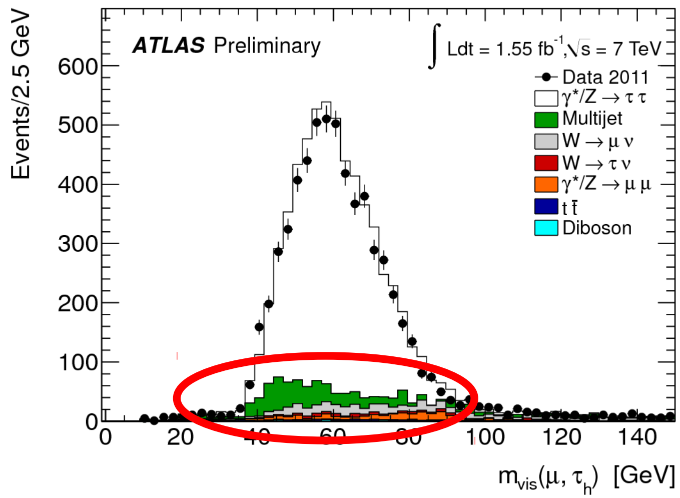

Z' → ττ search

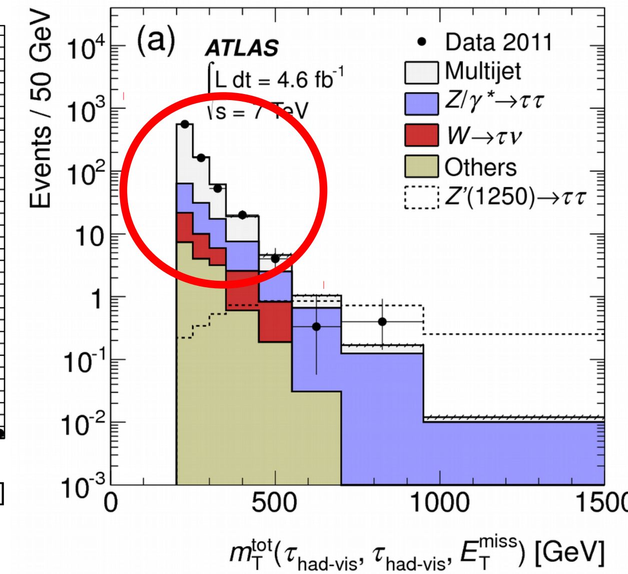

→ Fake τ's are major background:

Quark- or gluon-initiated jets

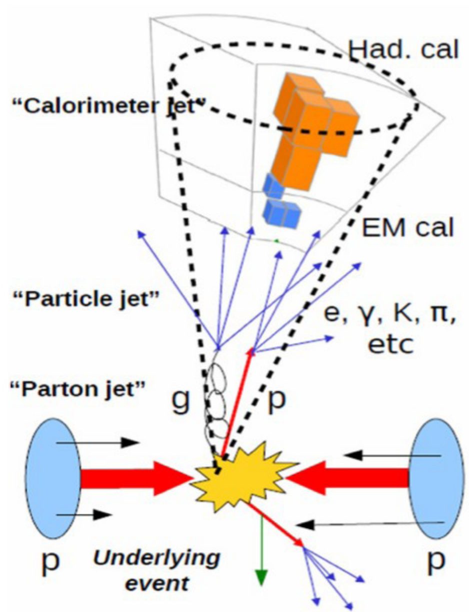

Jets fake τ's

→ Fake τ's are major background!

1) Huge QCD production cross section

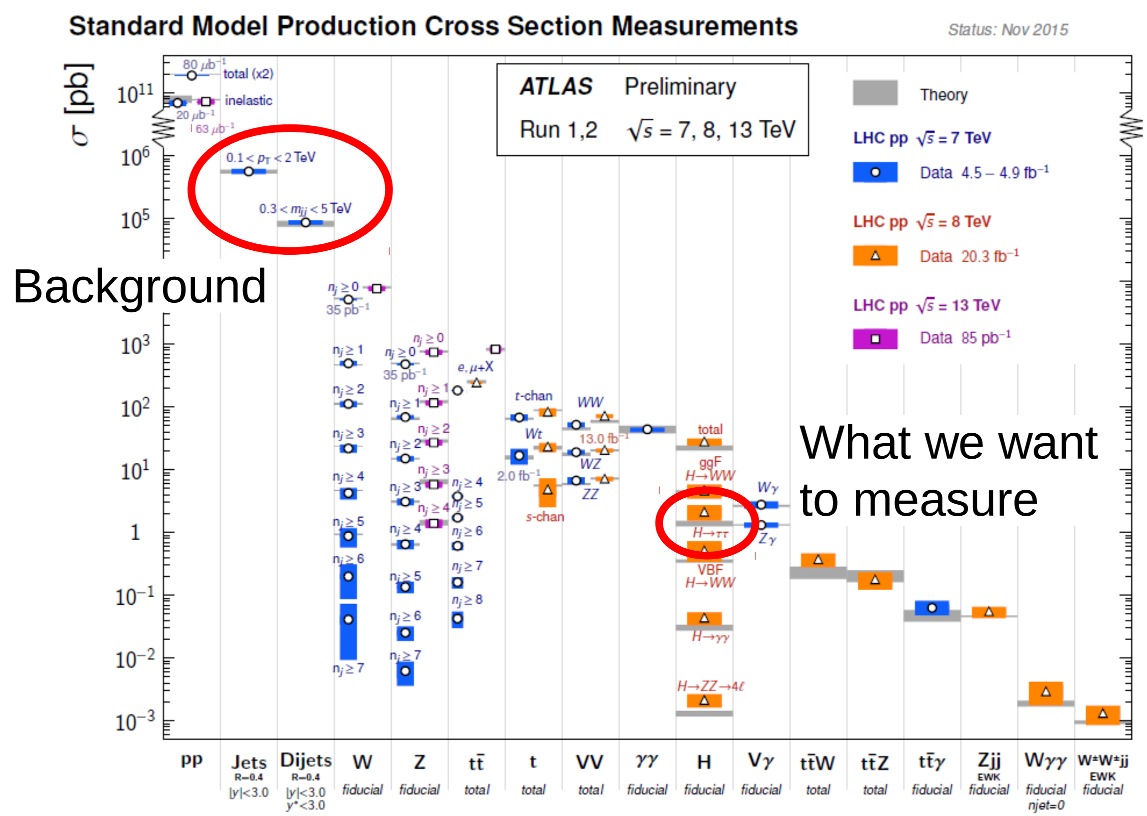

Jets fake τ's

→ Fake τ's are major background!

1) Huge QCD production cross section

2) QCD jets look similar

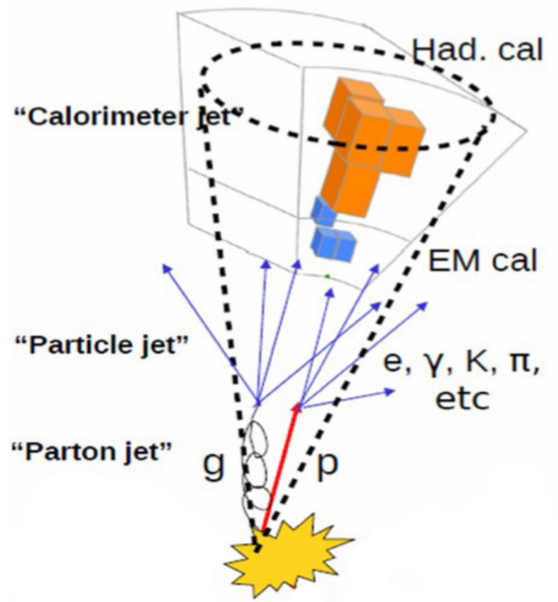

- Jets hadronize mostly into
  - $\pi^{\pm}$ (~60% of jet energy)
  - γ (~30%, from π^0)
  - Neutral hadrons (~10%)

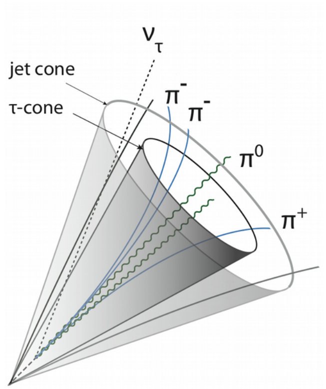

- Hadronically decaying taus (τ) decay almost exclusively into
  - $\pi^{\pm}$ (~100% of decays)
  - π^0 (~2/3 of decays)

Higgs analysis with τ's – Requirements

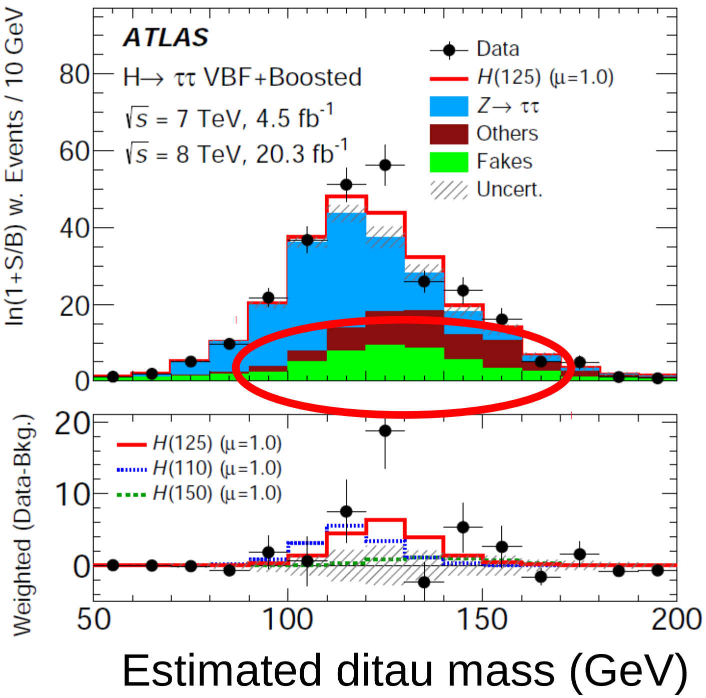

Fake τ's are major background:

- Large QCD cross section
- Jets "look similar" → hadronize into majorly pions

⇒ Need good discrimination against jets

Jet rejection factor ~100 achieved with excellent Run 1 tau identification:

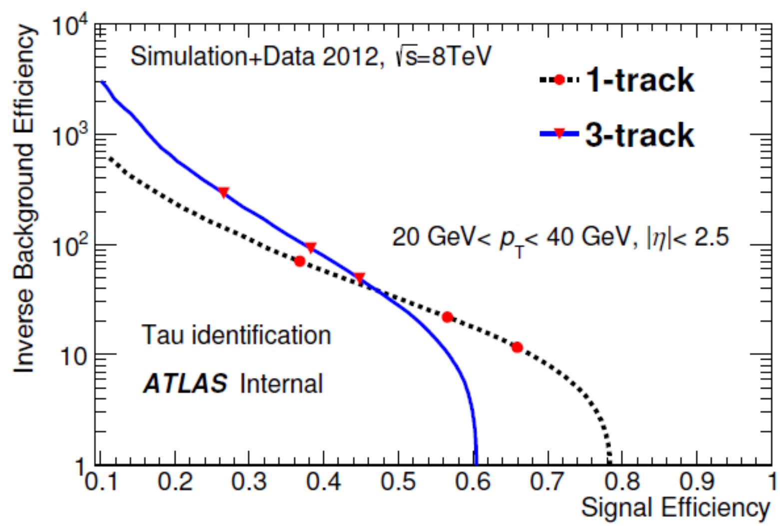

Tau Reco and ID efficiencies

Decay mode	$\mathcal{B}$ [%]	$\mathcal{A} \cdot \varepsilon_{\text{reco}}$ [%]	ε_{ID} [%]
$h^{\pm}$	11.5	32	75
$h^{\pm}\,\pi^0$	30.0	33	55
$h^{\pm} \geq 2\pi^0$	10.6	43	40
$3h^{\pm}$	9.5	38	70
$3h^{\pm} \geq 1\pi^0$	5.1	38	46

Table 2: Five dominant $\tau_{\text{had-vis}}$ decay modes [59]. Tau neutrinos are omitted from the table. The symbol $h^{\pm}$ stands for $\pi^{\pm}$ or $K^{\pm}$. Decays involving $K^{\pm}$ contribute ~3% to the total hadronic branching fraction. Decays involving neutral kaons are excluded. The branching fraction ($\mathcal{B}$), the fraction of generated $\tau_{\text{had-vis}}$'s in simulated $Z \to \tau\tau$ events that are reconstructed and pass the $\tau_{\text{had-vis}}$ selection described in Section 2.2 without the jet and electron discrimination ($\mathcal{A}\cdot\varepsilon_{\text{reco}}$) and the fraction of those $\tau_{\text{had-vis}}$ candidates that also pass the jet and electron discrimination (ε_{ID}) for each decay mode are given.

Tau Identification

- Reconstructed from energy deposits in calorimeter – initial steps identical to jet reconstruction
- Associate tracks reconstructed in the tracking detectors
- Identification using calorimeter cell and track variables: exploit that taus are on average more narrow than jets – excellent rejection of jets reaching factors of ~100!

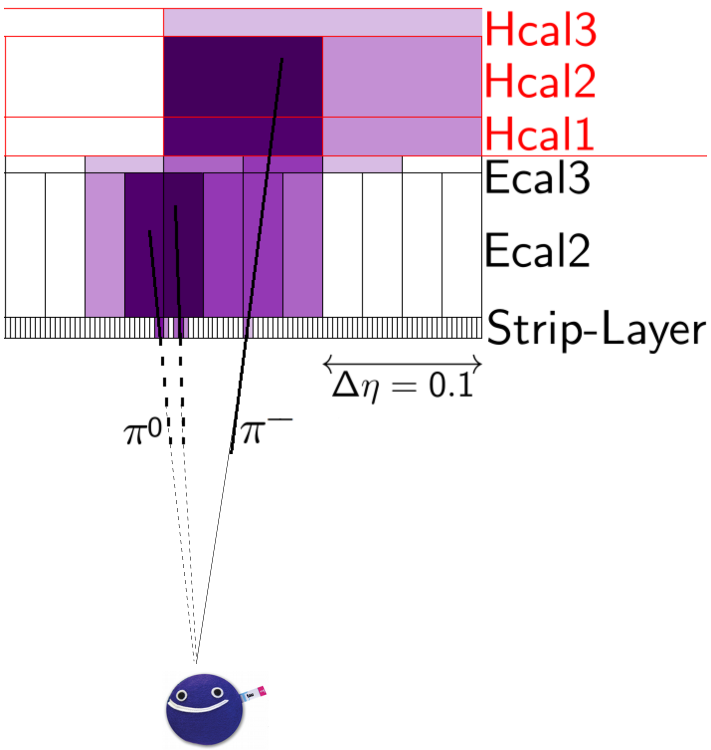

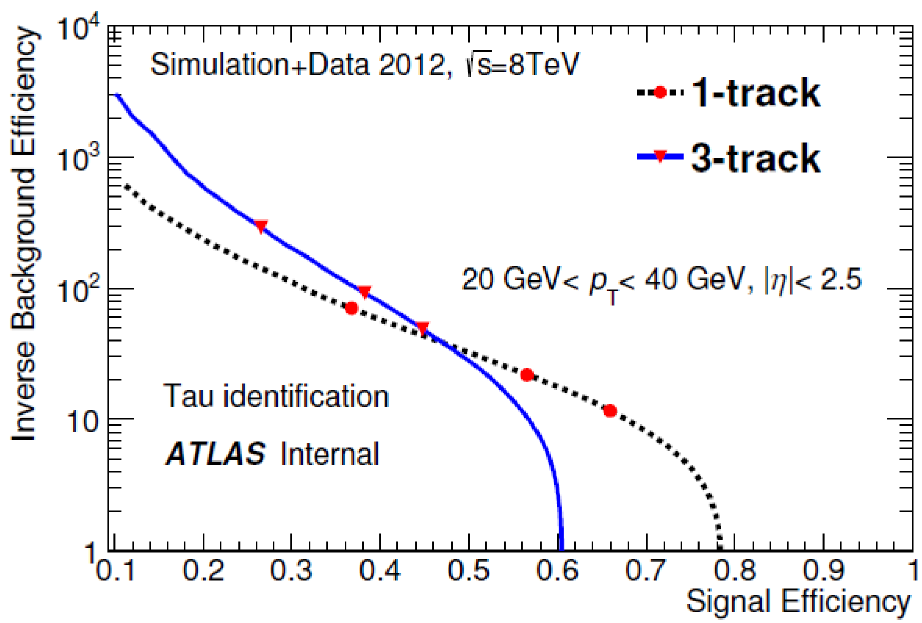

Reconstruction Algorithm

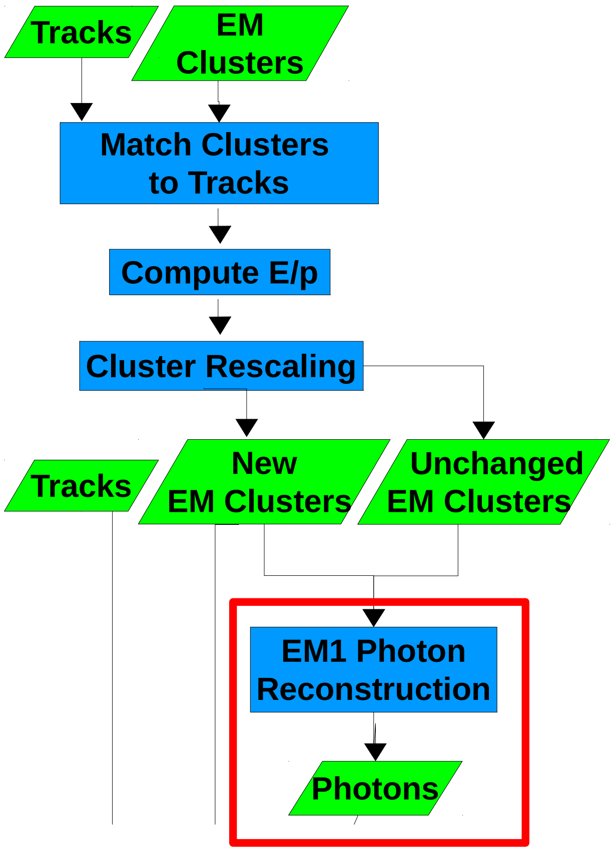

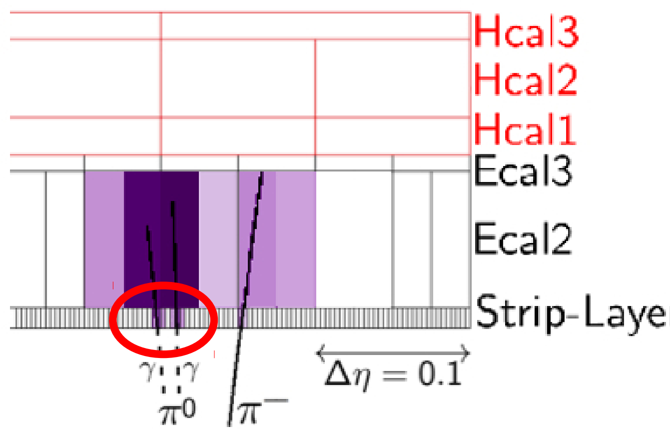

→ Tells us if a cluster contains more than 1 π^0

Counts energy deposits with E_T > 300-430 MeV associated to cluster, count twice if E_T > 10 GeV – improves

- Purity of decays with 1 π^0
- Efficiency of decays with 2 π^0

Reconstruction Algorithm

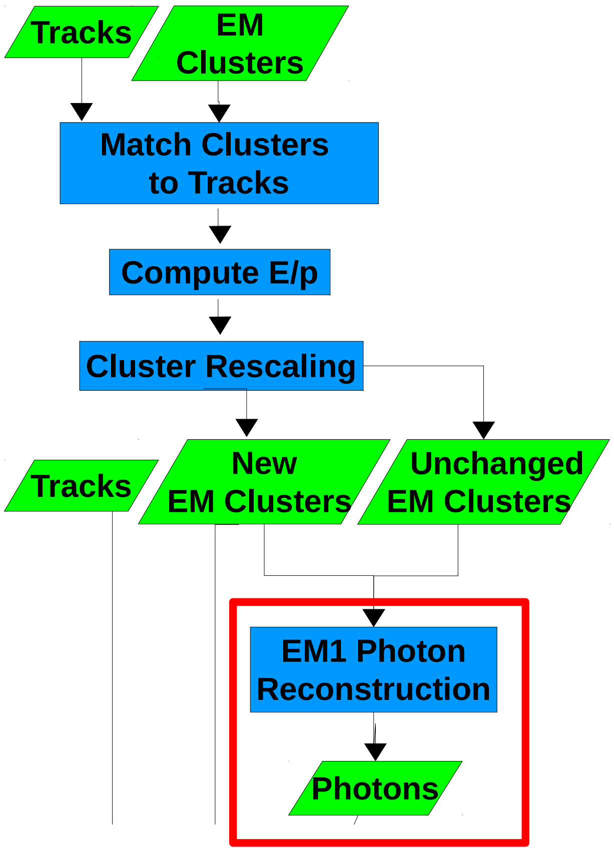

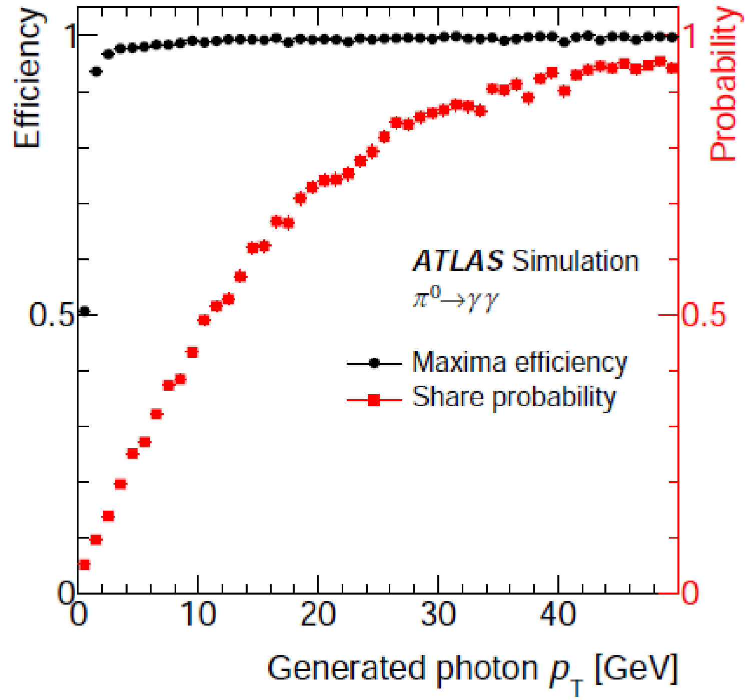

→ Tells us if a cluster contains more than 1 π^0

Counts energy deposits with E_T > 300-430 MeV associated to cluster, count twice if E_T > 10 GeV – improves

- Purity of decays with 1 π^0
- Efficiency of decays with 2 π^0

τ Performance: π^0 4-vector resolution

Angular core resolution: (0.0056, 0.012) in (η,ϕ)

Relative energy core resolution: 16%

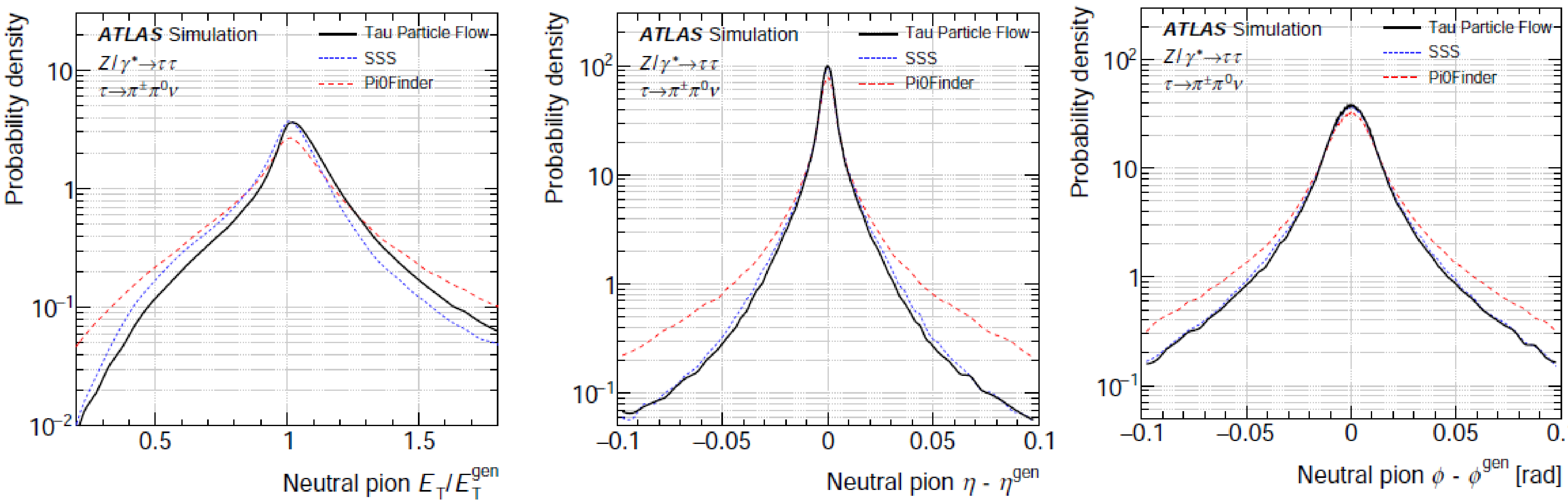

Pileup has very little impact **without pileup correction**!

- E_T increases by ~15 MeV per vertex
- E_T resolution degrades by 0.5% per vertex

τ Performance: Decay mode classification

Overall classification efficiency: 74.4%

- High efficiencies in important modes 1p0n, 1p1n and 3p0n
- High purity these modes (cf. Run 1 track-based classification: 27%, 52%, 69%)

Efficiency:

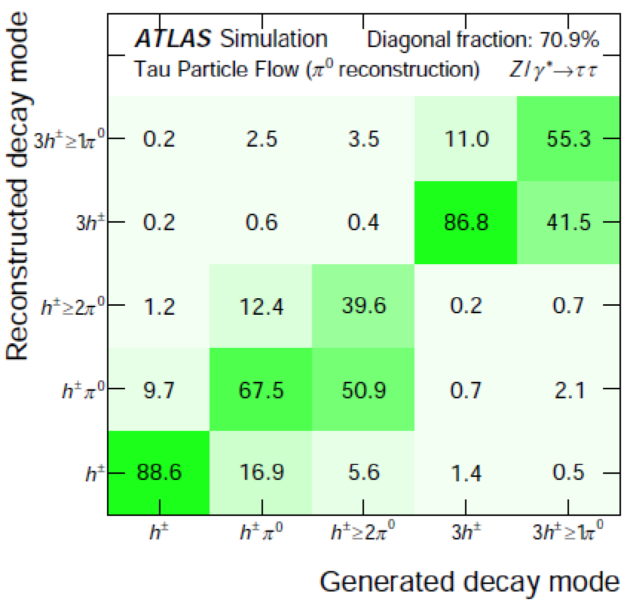

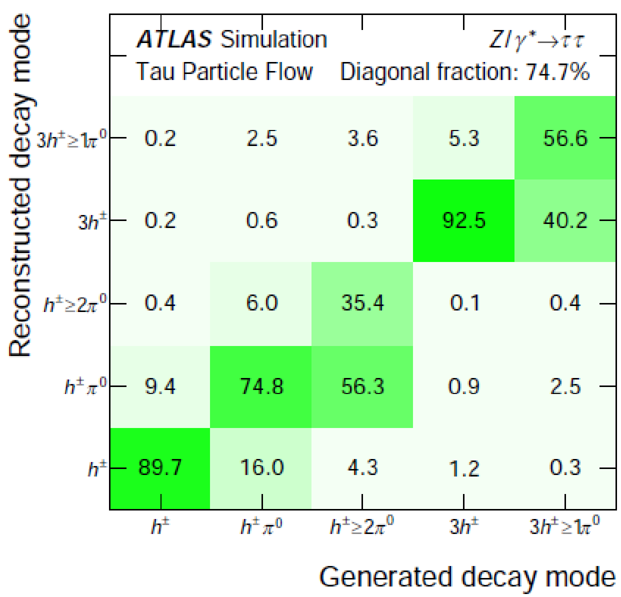

Purity:

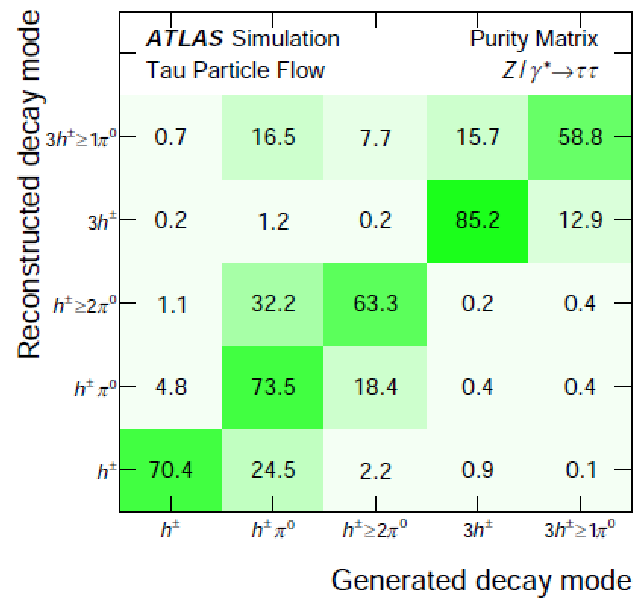

Little impact from pileup: efficiency degrades by ~0.04% per vertex

τ Performance: τ_{vis} 4-vector resolution

E_T response:

• Calculate resolution-weighted sum of "constituent-based" and calorimeter-only (= Run 1) E_T → smooth transition at high E_T where calorimeter measurement gets better

• To suppress E_T resolution tails → use Run 1 E_T if the two E_T disagree by >5σ

→ Rel. E_T core resolution ~8% at 20 GeV (Factor ~2 better than Run 1)

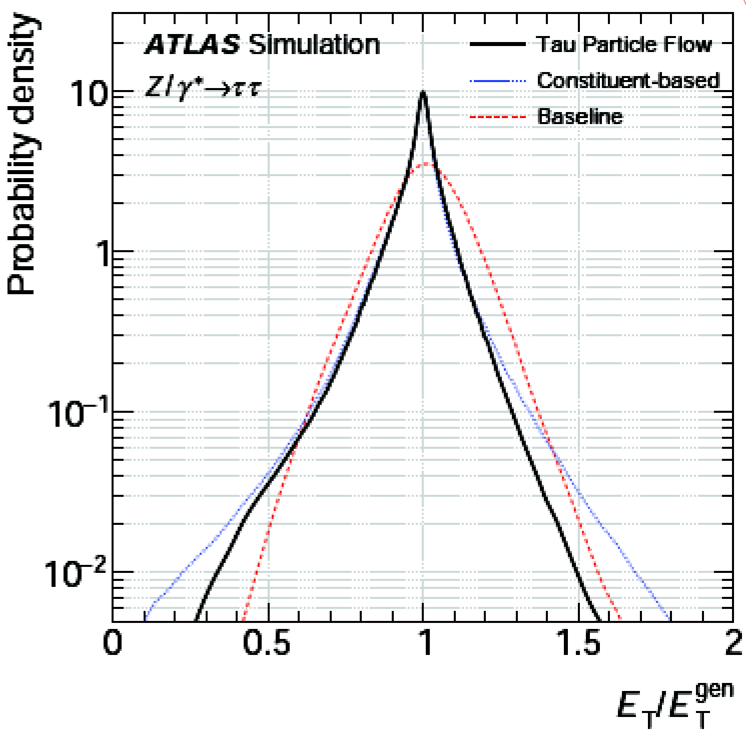

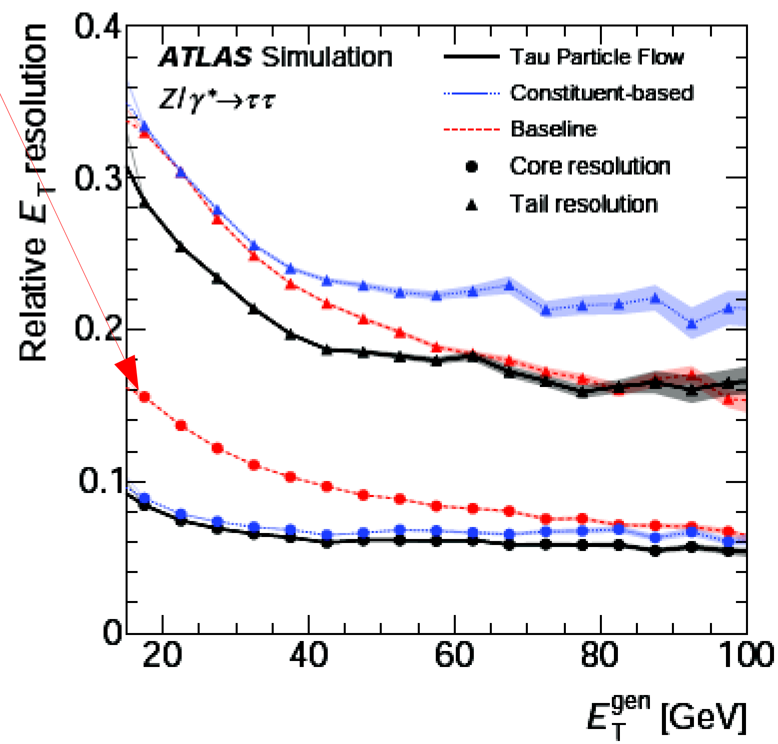

τ Performance: τ_{vis} 4-vector resolution

E_T response:

• Calculate resolution-weighted sum of “constituent-based” and calorimeter-only (= Run 1) E_T → smooth transition at high E_T where calorimeter measurement gets better

• To suppress E_T resolution tails → use Run 1 E_T if the two E_T disagree by >5σ

→ Rel. E_T core resolution ~8% at 20 GeV (Factor ~2 better than Run 1)

Little impact from pileup **without pileup correction**:

• E_T increases by ~4 MeV per vertex

• Resolution degrades by ~0.5%

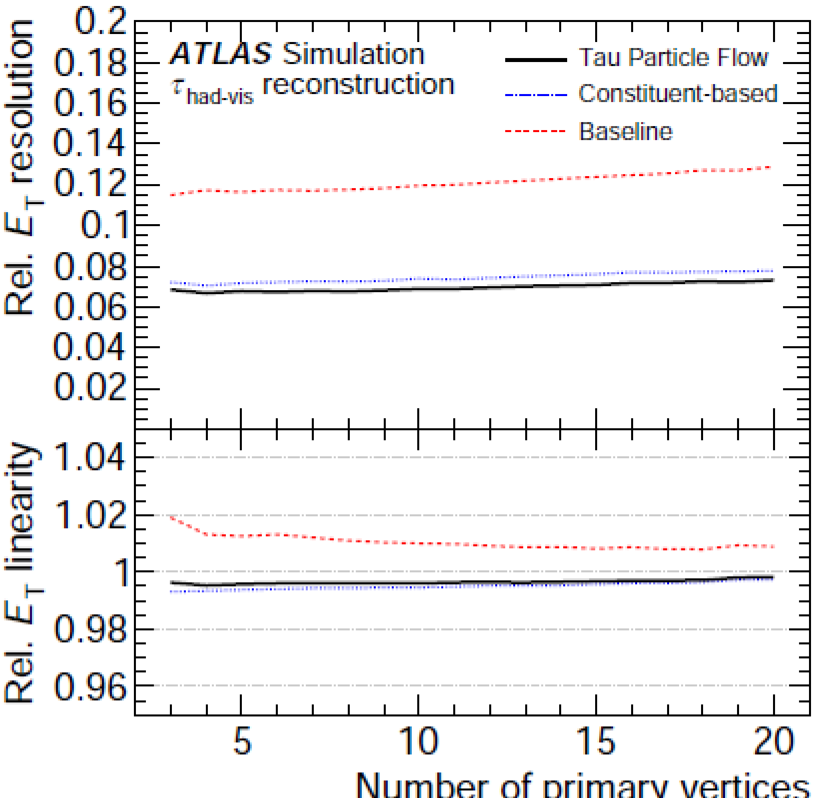

τ Performance: π^0 ID

Cluster pseudorapidity, $|\eta^{\text{clus}}|$
Magnitude of the energy-weighted η position of the cluster

Cluster width, $\langle r^2 \rangle^{\text{clus}}$
Second moment in distance to the shower axis

Cluster η width in EM1, $\langle \eta^2_{\text{EM1}} \rangle^{\text{clus}}$
Second moment in η in EM1

Cluster η width in EM2, $\langle \eta^2_{\text{EM2}} \rangle^{\text{clus}}$
Second moment in η in EM2

Cluster depth, $\lambda^{\text{clus}}_{\text{centre}}$
Distance of the shower centre from the calorimeter front face measured along the shower axis

Cluster PS energy fraction, $f^{\text{clus}}_{\text{PS}}$
Fraction of energy in the PS

Cluster core energy fraction, $f^{\text{clus}}_{\text{core}}$
Sum of the highest cell energy in PS, EM1 and EM2 divided by the total energy

Cluster logarithm of energy variance, $\log\langle \rho^2 \rangle^{\text{clus}}$
Logarithm of the second moment in energy density

Cluster EM1 core energy fraction, $f^{\text{clus}}_{\text{core,EM1}}$
Energy in the three innermost EM1 cells divided by the total energy in EM1

Cluster asymmetry with respect to track, $\mathcal{A}^{\text{clus}}_{\text{track}}$
Asymmetry in η–ϕ space of the energy distribution in EM1 with respect to the extrapolated track position

Cluster EM1 cells, $N^{\text{clus}}_{\text{EM1}}$
Number of cells in EM1 with positive energy

Cluster EM2 cells, $N^{\text{clus}}_{\text{EM2}}$
Number of cells in EM2 with positive energy

τ Performance: π^0 ID

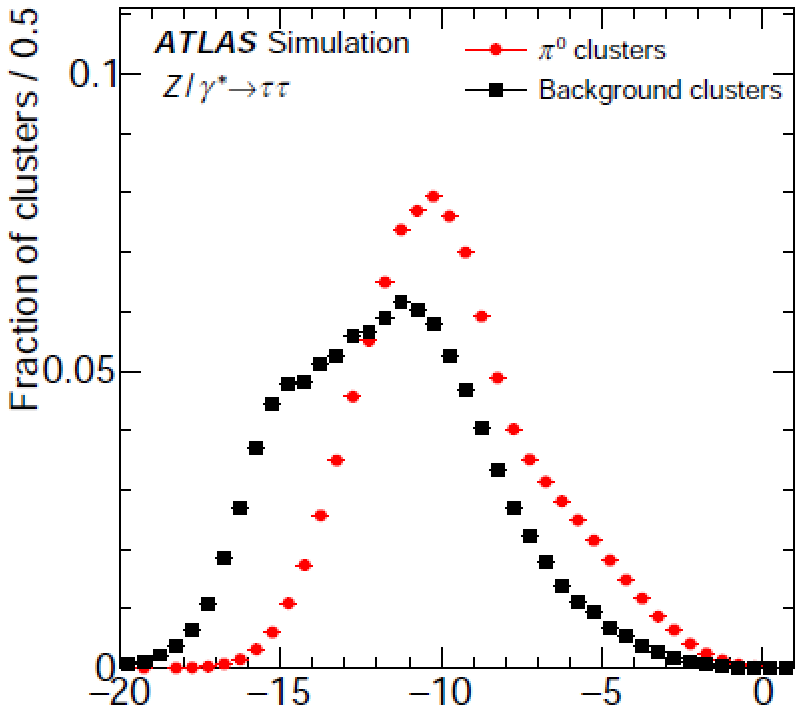

(a)

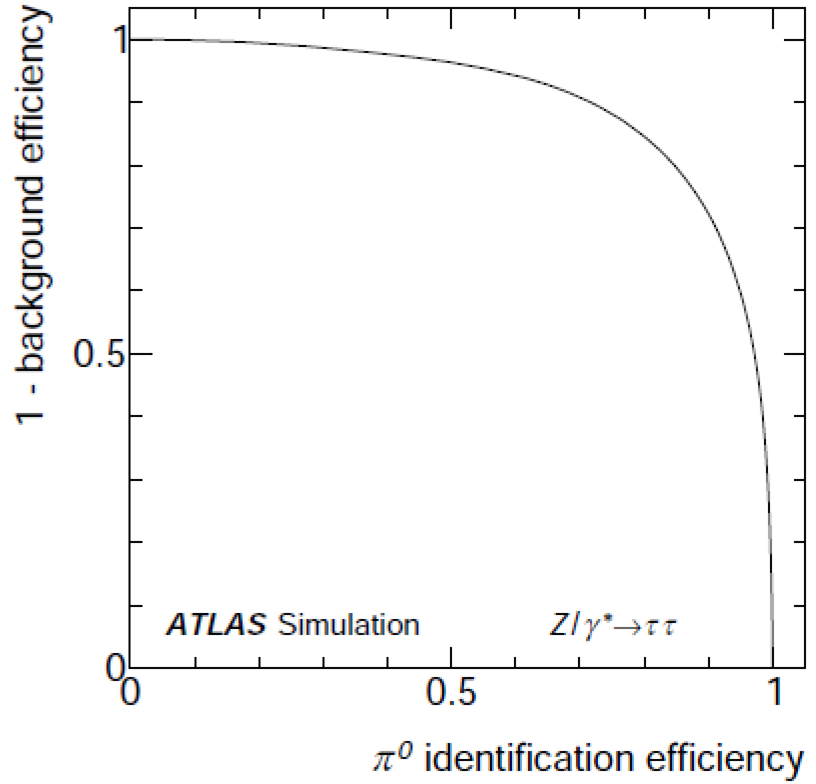

(b)

Figure 1: (a) Distribution of the logarithm of the second moment in energy density of π^0_{cand} clusters that do (signal) or do not (background) originate from π^0's, as used in the π^0 identification. (b) 1 – efficiency for background π^0_{cand}'s vs. the efficiency for signal π^0_{cand}'s to pass thresholds on the π^0 identification score. The π^0_{cand}'s in both figures are associated with $\tau_{\text{had-vis}}$'s selected from simulated $Z \to \tau\tau$ events.

τ Performance: ECAL1 deposits

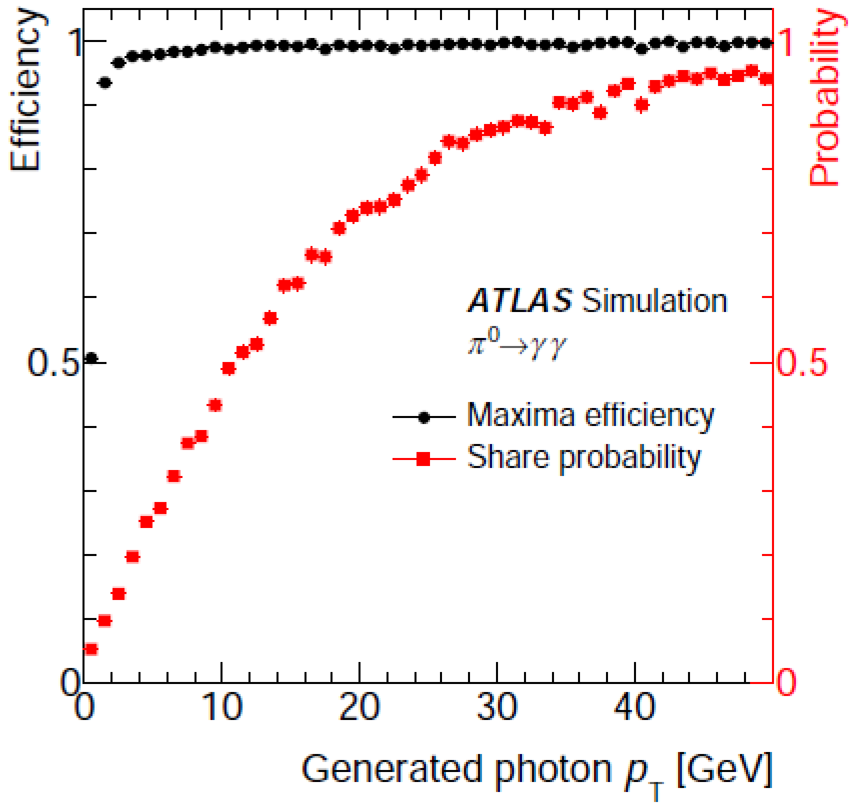

Figure 4: Efficiency for a photon to create a maximum in the first layer of the EM calorimeter in simulated $\pi^0 \rightarrow \gamma\gamma$ events and the corresponding probability to create a maximum that is shared with the other photon. The photons are required to not interact with the material in the tracking system.

τ Performance: Kinematic decay mode classification

π^0 identification score of the first π^0_{cand}, S_1^{BDT}
π^0 identification score of the π^0_{cand} with the highest π^0 identification score

E_{T} fraction of the first π^0_{cand}, $f_{\pi^0,1}$
E_{T} of the π^0_{cand} with the highest π^0 identification score, divided by the E_{T}-sum of all π^0_{cand}'s and $h^{\pm}$'s

Hadron separation, $\Delta R(h^{\pm}, \pi^0)$
ΔR between the $h^{\pm}$ and the π^0_{cand} with the highest π^0 identification score

$h^{\pm}$ distance, $D_{h^{\pm}}$
E_{T}-weighted ΔR between the $h^{\pm}$ and the $\tau_{\text{had-vis}}$ axis, which is calculated by summing the four-vectors of all $h^{\pm}$'s and π^0_{cand}'s

Number of photons, N_{γ}
Total number of photons in the $\tau_{\text{had-vis}}$, as reconstructed in Section 3.3

π^0 identification score of second π^0_{cand}, S_2^{BDT}
π^0 identification score of the π^0_{cand} with the second-highest π^0 identification score

π^0_{cand} E_{T} fraction, f_{π^0}
E_{T}-sum of π^0_{cand}'s, divided by the E_{T}-sum of π^0_{cand}'s and $h^{\pm}$'s

π^0_{cand} mass, m_{π^0}
Invariant mass calculated from the sum of π^0_{cand} four-vectors

Number of π^0_{cand}, N_{π^0}

Standard deviation of the $h^{\pm}$ p_{T}, $\sigma_{E_{\text{T}},h^{\pm}}$
Standard deviation, calculated from the p_{T} values of the $h^{\pm}$'s for $\tau_{\text{had-vis}}$ with three associated tracks

$h^{\pm}$ mass, $m_{h^{\pm}}$
Invariant mass calculated from the sum of $h^{\pm}$ four-vectors

τ Performance: Kinematic decay mode classification

Decay mode test	$N(\pi^0_{\text{cand}})$	$N(\pi^0_{\text{ID}})$	Variables
$h^\pm\{0,1\}\pi^0$	≥ 1 1	0 1	S_1^{BDT}, $f_{\pi^0,1}$, $\Delta R(h^\pm,\pi^0)$, $D_{h^\pm}$, N_γ
$h^\pm\{1,\geq 2\}\pi^0$	≥ 2 ≥ 2	1 ≥ 2	S_2^{BDT}, f_{π^0}, m_{π^0}, N_{π^0}, N_γ
$3h^\pm\{0,\geq 1\}\pi^0$	≥ 1 ≥ 1	0 ≥ 1	S_1^{BDT}, f_{π^0}, $\sigma_{E_{\text{T}},h^\pm}$, $m_{h^\pm}$, N_γ

Table 5: Details regarding the decay mode classification of the Tau Particle Flow. BDTs are trained to distinguish decay modes in three decay mode tests. The $\tau_{\text{had-vis}}$'s entering each test are further categorised based on the number of reconstructed, $N(\pi^0_{\text{cand}})$, and identified, $N(\pi^0_{\text{ID}})$ neutral pions. The variables used in the BDTs for each test are listed.

τ Performance: Kinematic decay mode classification

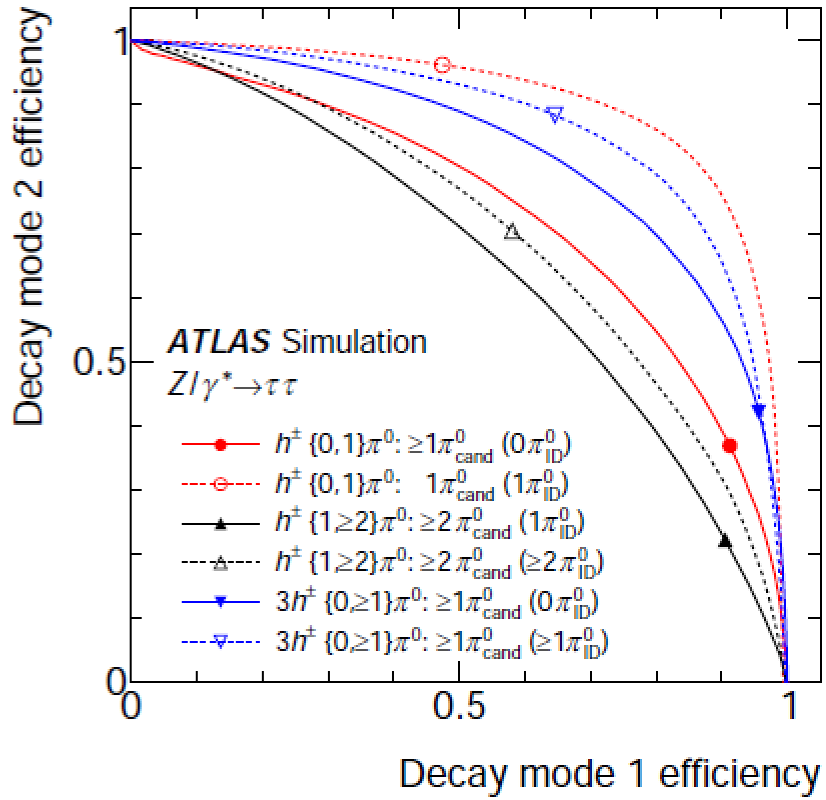

Figure 5: Decay mode classification efficiency for the $h^{\pm}\{0,1\}\pi^0$, $h^{\pm}\{1,\geq 2\}\pi^0$, and $3h^{\pm}\{0,\geq 1\}\pi^0$ tests. For each test, "decay mode 1" corresponds to the mode with fewer π^0's. Working points corresponding to the optimal thresholds on the BDT score for each test are marked.

What's the gain? – H vs. Z discrimination

Discriminate

Z (vector)

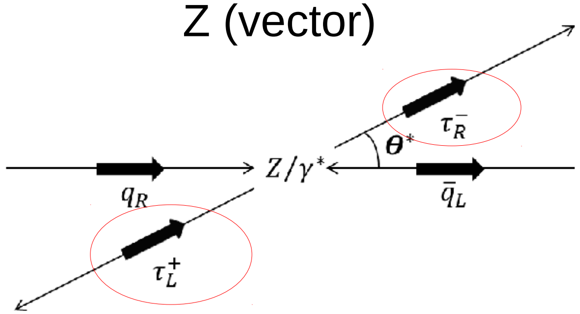

H (scalar)

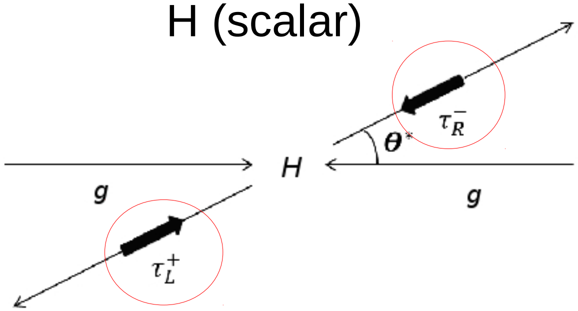

Longitudinal τ polarization

Discrimination through correlation of π^-– π^0 energy asymmetry

Prerequisites:

- Need to reconstruct π^0 energy
- High purity decay mode classification

→ Now available with new reconstruction

ATLAS Run 1 Tau Reconstruction

- τ_h appears as narrow, isolated jet from neutral (e.g. π^0) and charged particles (e.g. $\pi^\pm$)
- Calorimeter seed: anti-kT jet with R=0.4, p_T > 10 GeV, |η|<2.5
- Classify in number of tracks ("prongs") in ΔR=0.2 of jet seed
- τ_h energy = energy of topological clusters within ΔR=0.2

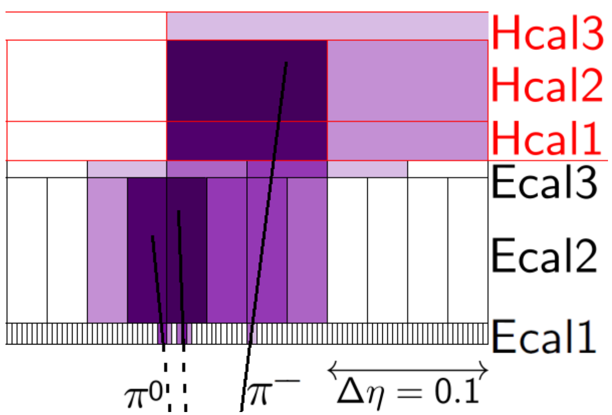

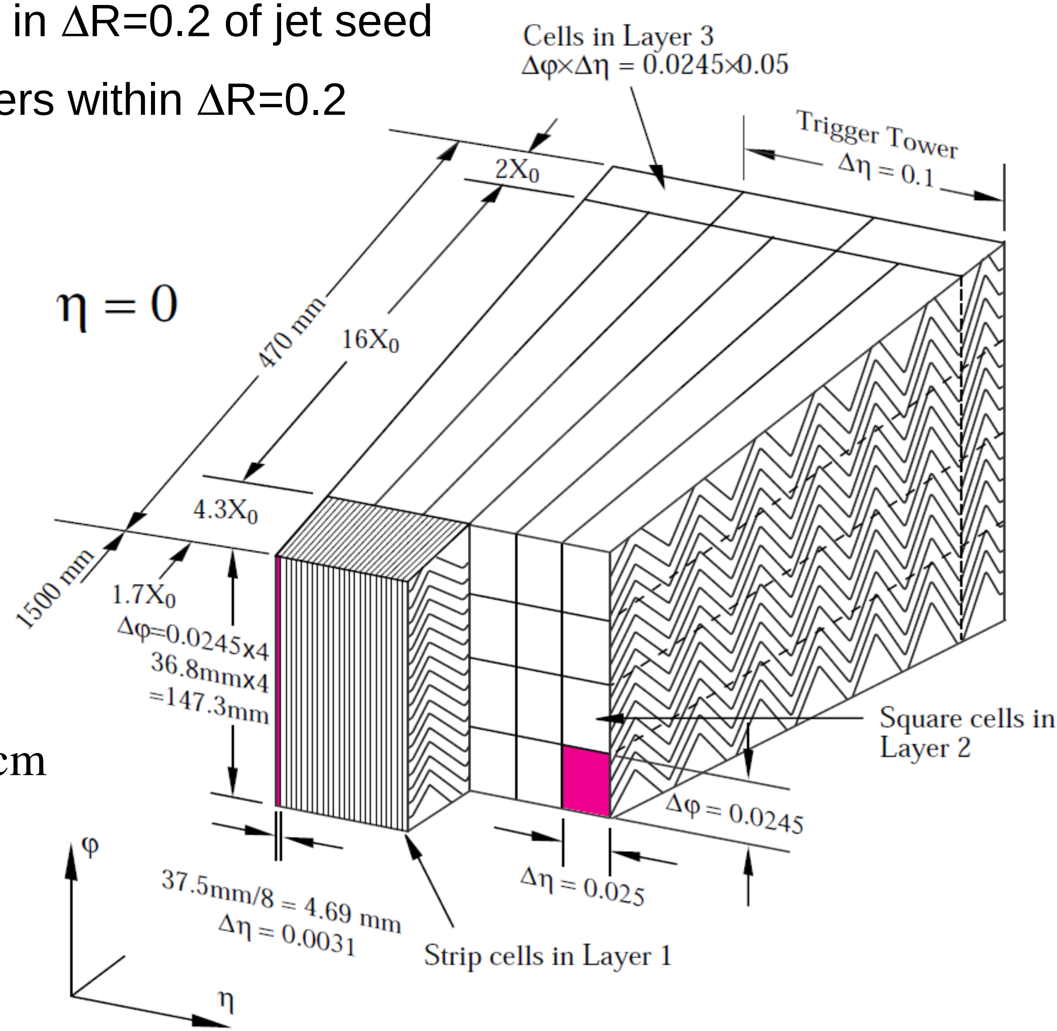

ECAL: X_0 ~ 2.1 cm, Molière radius ~ 4.4 cm

HCAL: 0.1x0.1 in η/ϕ, 7.4λ long, 3 layers

ATLAS Run 1 Tau Reconstruction

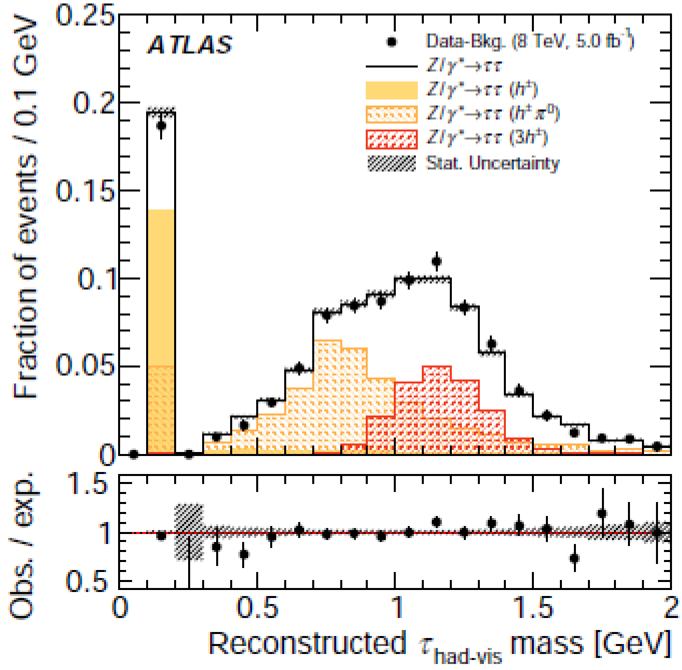

Figure 13: Distribution of the reconstructed mass of the $\tau_{\mathrm{had-vis}}$ when using the Tau Particle Flow $\tau_{\mathrm{had-vis}}$ four-momentum reconstruction in the $Z \rightarrow \tau\tau$ tag-and-probe analysis. The estimated background contribution, dominated by multijet and $W(\rightarrow \mu\nu)$+jets production, has been subtracted from the data. The simulated $Z \rightarrow \tau\tau$ sample is normalised to the background subtracted data. The contributions from $\tau_{\mathrm{had-vis}}$ with generated $h^{\pm}$, $h^{\pm}\,\pi^{0}$ and $3h^{\pm}$ modes are overlaid. The hatched band represents the statistical uncertainty on the prediction.

ATLAS Run 1 Tau Reconstruction

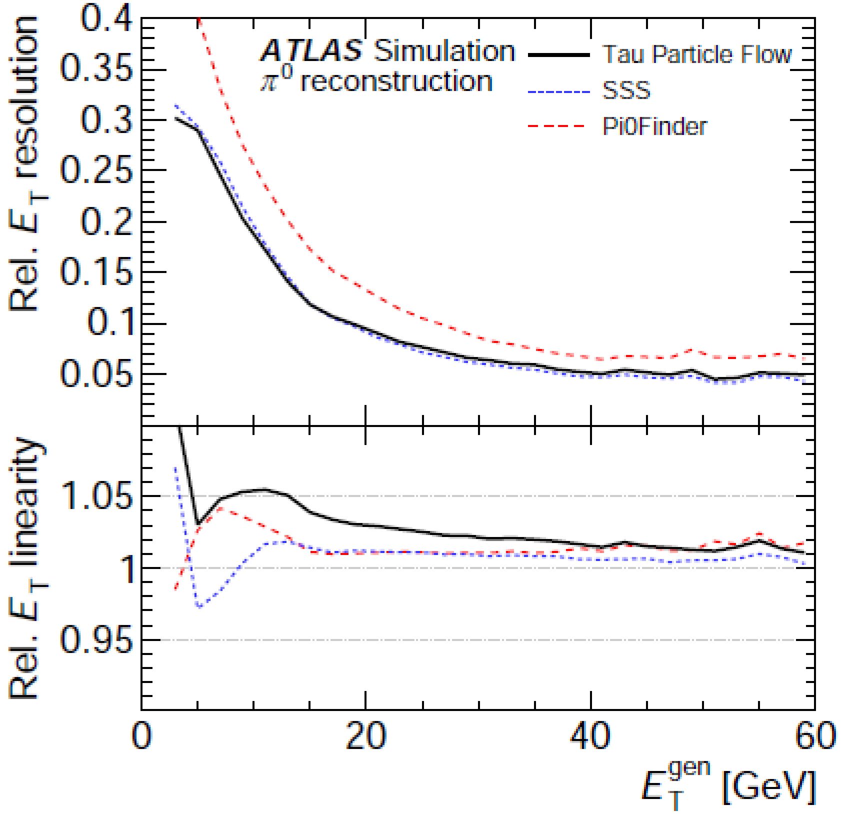

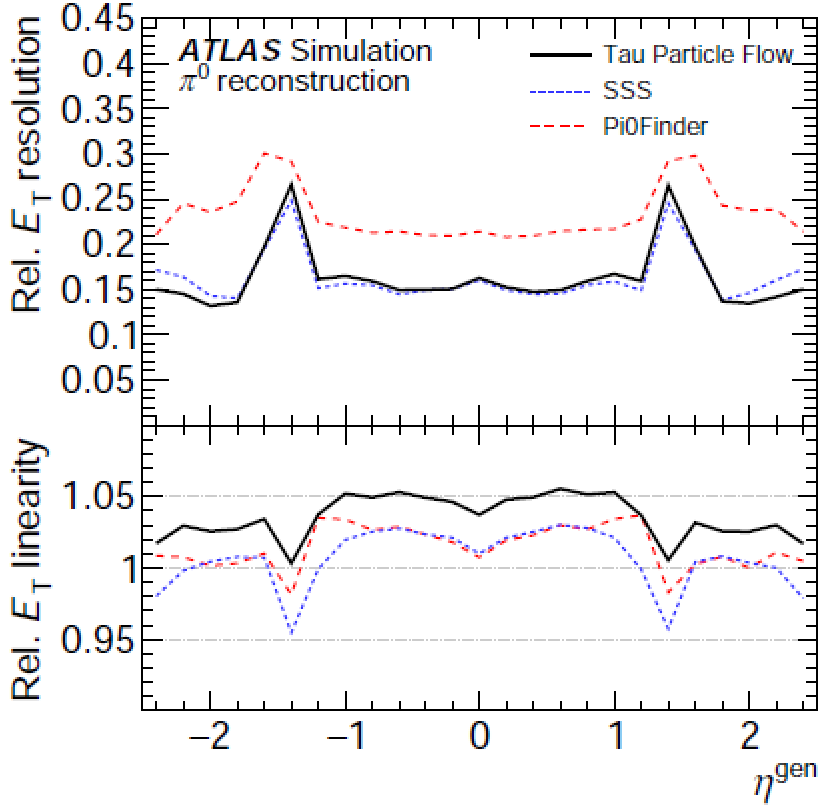

ATLAS Run 1 Tau Reconstruction

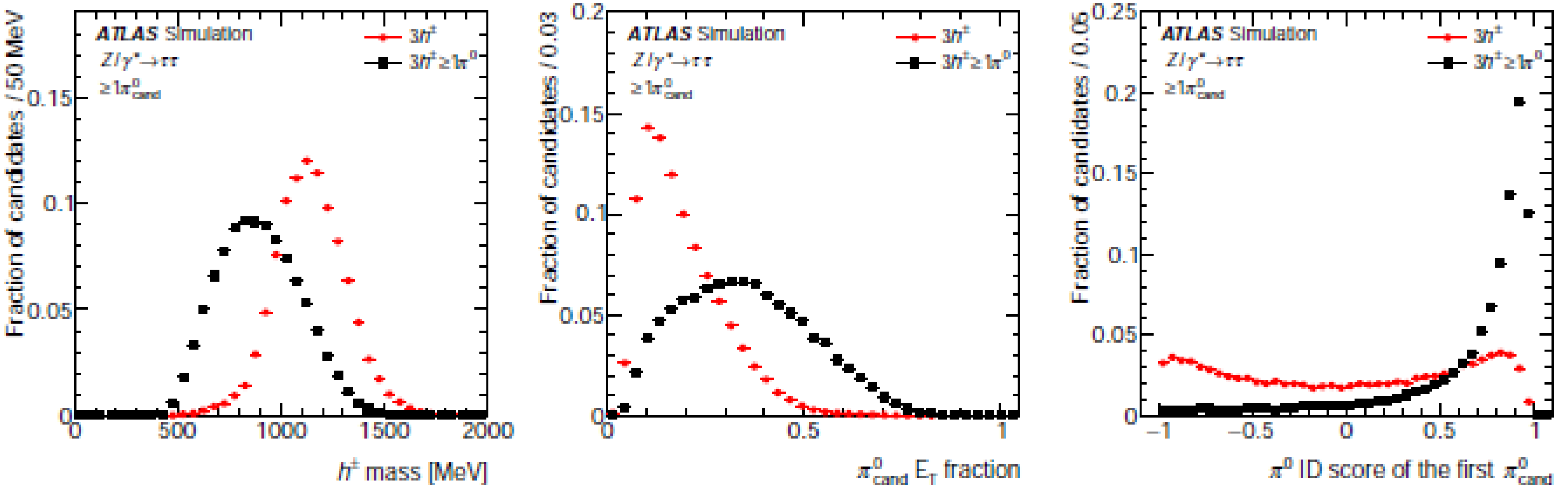

(a) (b) (c)

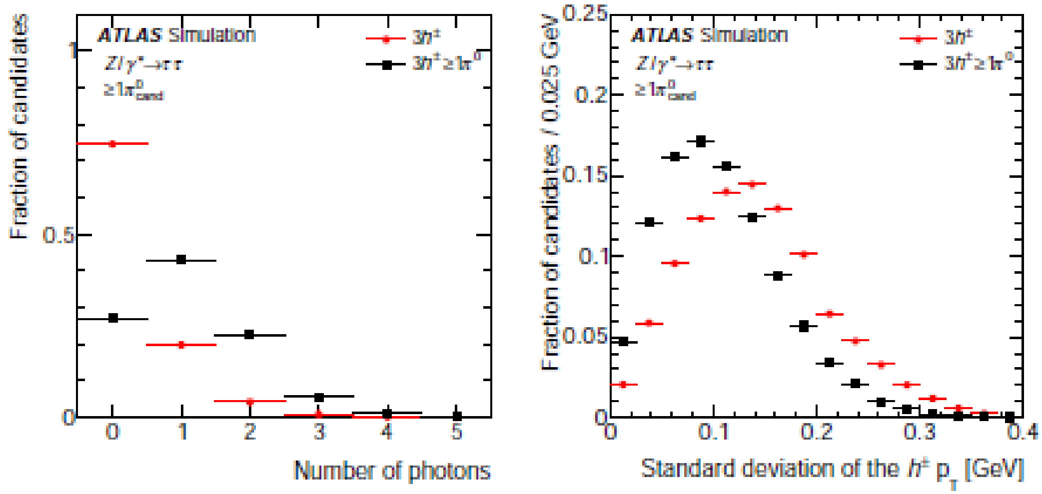

ATLAS Run 1 Tau Reconstruction

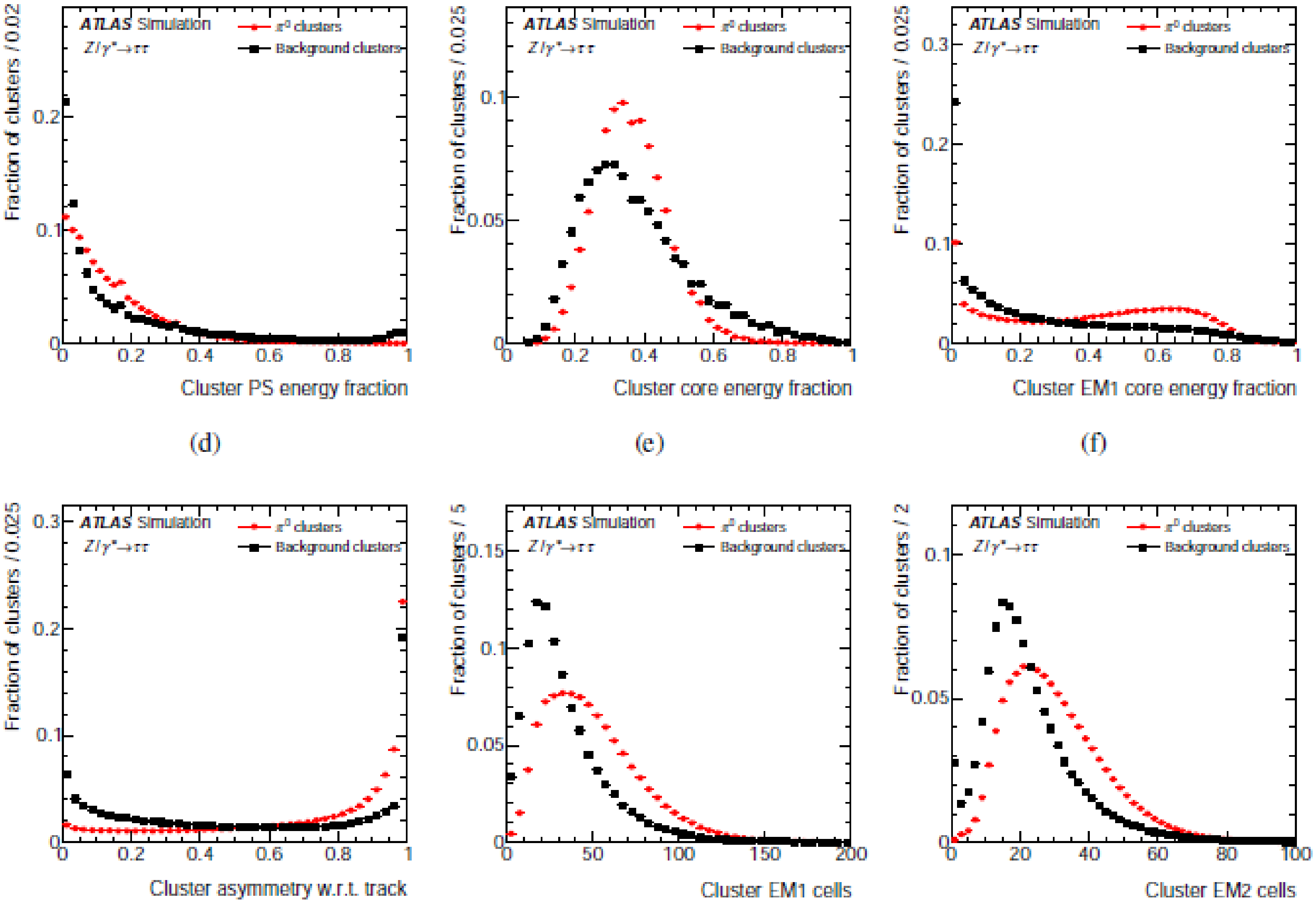

ATLAS Run 1 Tau Reconstruction

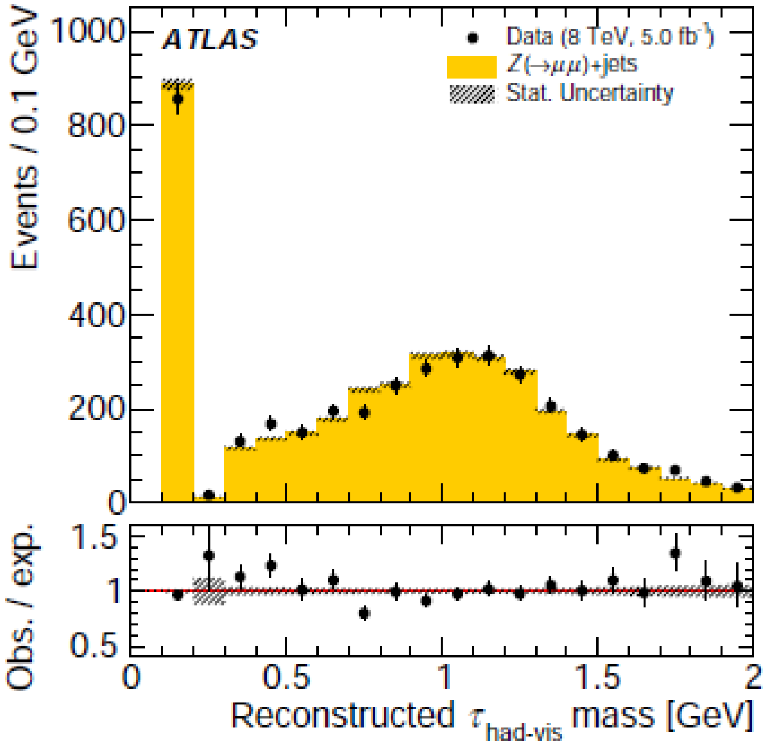

Figure 11: Tau m_{vis} distribution of the Tau Particle Flow reconstruction of fake tau candidates from jets in a $Z(\rightarrow \mu\mu)$+jets event selection, for data and simulation. The simulated $Z(\rightarrow \mu\mu)$+jets events are reweighted so that the Z boson p_T distribution and the overall normalisation match that in the data. The hatched band represents the statistical uncertainty on the prediction.

ATLAS Run 1 Tau Reconstruction